PEOPLE'S DEMOCTRATIC REPUBLIC OF ALGERIA

Ministry of Higher Education and Scientific Research

Serial N°: ……/2024

University of Kasdi Merbah Ouargla

Faculty of Hydrocarbons, Renewable Energies, Earth and Universe Sciences

Department of Drilling & Petroleum Fields Mechanics

Dissertation

To obtain the Master's degree
Option: Professional Drilling

Submitted by:

Menakh Ouassim, Yagoub Kheireddine Hazem, Bouchelouche Amine

- THEME-

COMPARAISON BETWEEN COMMERCIAL SOFTWARE AND SELF-ROLLED PERFORMANT PROGRAM IN PRIMARY CEMENTING JOB

Defended on:

Jury :

Presedent :	**Bellofi Youcef**	Univ. Ouargla
Supervisor:	**Abidi-Saad Elfaker**	Univ. Ouargla
Examiner :	**Merabti Houcine**	Univ. Ouargla

Academic Year: 2023/2024

Dedication

"By The Name of God most Gracious most merciful "

All prize is to Allah, for guiding us through our study journey and through all our life.

A big thank to all our family members and all our friends.

Special gratitude to our parents for their mental and financial support.

Acknowledgement

This dissertation would not have been possible without the invaluable support and guidance of several individuals. I would like to express my sincere gratitude to:

Mentor Abidi-saad Elfaker: Your unwavering support and encouragement throughout this journey have been a constant source of motivation. I am grateful for your patience, feedback, and dedication to my success.

: Thank you for your technical expertise and willingness to share your knowledge throughout this project. Your insights and guidance were instrumental in shaping my understanding of the field and overcoming technical challenges. I am truly fortunate to have had such a supportive network during this endeavor

Abstract

Drilling a well is more then just penetrate some thousands of meters. In fact, the well should be in good conditions through cementing, and to prevent danger consequences of bad cementing, a good design should be done prior the job and correct decisions should be taken in the field.

Technology development allows engineers to imagine future results and make suitable changes if necessary to guarantee the success of the process and estimate the challenges by combining the fluid mechanic proved rules and schematic illustrations of the computer programs.

Key words: Flow regimes, flow rates, equivalent circulating density **ECD**, compatibility, top of cement **TOC**.

Résumé

Le forage d'un puits, ce n'est pas simplement pénétrer quelques milliers de mètres. En fait, le puits doit être dans de bonnes conditions grâce à la cimentation, et pour éviter les conséquences dangereuses d'une mauvaise cimentation, une bonne design doit être réalisée avant le travail et des décisions correctes doivent être prises sur le terrain.

Le développement technologique permet aux ingénieurs d'imaginer les résultats futurs et d'apporter les modifications appropriées si nécessaire pour garantir le succès du processus et estimer les défis en combinant les règles éprouvées de la mécanique des fluides et les illustrations schématiques des programmes récentes

Mots clés : Régimes d'écoulement, débits, densité circulante équivalente **ECD**, compatibilité, Top of Cement **TOC**.

الملخص

إن حفر بئر هو أكثر من مجرد اختراق بضعة آلاف من الأمتار. في الواقع، يجب أن تكون البئر في حالة جيدة من خلال التدعيم ببطانة من الاسمنت، ولمنع عواقب خطر سوء التدعيم، يجب عمل تصميم جيد قبل العمل ويجب اتخاذ القرارات الصحيحة في الميدان.

يتيح تطوير التكنولوجيا للمهندسين تصور النتائج المستقبلية وإجراء التغييرات المناسبة إذا لزم الأمر لضمان نجاح العملية وتقدير التحديات من خلال الجمع بين القواعد المثبتة لميكانيكا الموائع والرسوم التوضيحية التخطيطية لبرامج الكمبيوتر الحديثة.

الكلمات المفتاحية: أنظمة التدفق، معدلات التدفق، كثافة التدوير المكافئة

Table of content

List of figures

List of tables

List of abbreviations

API American Petroleum Intuits

BHP Bottom Hole Pressure

TOC Top Of Cement

CBL Cement Bond Log

VDL Variable-density log

T.T Thickening Time

BHST Bottom Hole Static Temperature

RPM Rotation Per Minute

HB Herschel-Bulkley

General introduction

As the demand for hydrocarbons continues to rise, the industry faces increasing challenges in drilling deeper, more complex wells while adhering to stringent environmental regulations. Cementing, therefore, comes to fulfil the drilling process and stands in as a critical barrier between the subsurface formations and the surface environment, safeguarding against potential hazards and ensuring operational excellence.

Cementing is one of the most critical operations in well planning, and it plays a pivotal role in ensuring the integrity and longevity of oil wells. Thus, it ensures the well stabilization and prevents many problems. Oil well cementing is a multifaceted process that encompasses various stages, each essential for the successful completion and production of a well. From casing support and zonal isolation to hydraulic fracturing containment and well abandonment, cementing operations are meticulously designed and executed to withstand extreme downhole conditions, including high pressures, temperatures, and corrosive environments. For a good cementing planning it is necessary to simulate the operation to get the optimum results along with minimizing common and particular issues.

In this project we take CemFACTS software as reference and attempt to develop piece of program to get better simulations which will be presented as graphs while several parameters have been taken on consideration. The first chapter provides an overview of well cementing, discussing the main objectives and presenting essential basics along with the general cementing procedure, to establish a clear foundation for the following chapters. The second chapter focuses on calculations, particularly fluid properties such as rheology and classification. All necessary theoretical formulas will be provided without extensive demonstrations, as they are widely accepted. The third chapter introduces our simulation, detailing the steps to select the best practices before executing the job in the field. The fourth chapter presents our results, comparing them with those from CemFACTS. We will also discuss the assumptions that may explain the differences between the results and offer our perspective for future students working on this project.

CHAPTER I

GENERALITIES ON WELL CEMENTATION

I.1 Introduction

The key to succeed in drilling a well is not just to reach the desired depth in the shortest time, indeed to maintain the hole stable and limit external forces and fluid migration in and out. For that, a casing string is run and cemented after drilling any phase (stage). selection a good casing and perfect length and strength is not able to consolidate the wellbore unless a good cementing job is applied.

Cementing in oil and gas wells is a necessary process thus it conserves the stability of wellbore. After running casing and fix it, a cements slurry is being prepared and pumped down the string up the annulus between formation and external casing, the slurry hardens and fill the gap. Making the well strong enough to resist internal pressures and provide a good isolation between formations that can provoke future problems, and strengthen the casing that guide hydrocarbons and drilling fluid to surface.

Drilling success should not be rated in terms of "penetration per hour", but more in terms of achieving a gauge hole. This is especially true for critical zones across permeable formations and/or salt sections. Care is required to prevent washouts during drilling of these formations. For achieving this, utmost care has to be given to the conditioning of drilling fluids.[1]

After preparing slurry and select the convenient cement type and correct additives and before start pumping, several laboratory tests should be done. The next subsequent will describe briefly the practical tests and their specific regulations.

Although all these regulations are respected, some challenges are always present. The last part of this chapter will discuss those issues.

After this chapter the reader will have a big picture on cementing job process and what are its main objectives, and its special considerations to succeed in the job and get better results.

I.2 Objectives

The main objective of cementing is to provide secure and safe situations to continue drilling and to organize a good path while production hydrocarbons by keeping the casing centered in its appropriate place.

Preventing gas migration or fluid connections between isolated zones and productive zones can prevent danger consequences e.g. aquifer leaks and soluble the salt formation (Houd berkaoui catastrophe of contamination of fresh water, dissolution of salt formations).

A solid structure would be offered to manipulate and practice tests in down hole safely and prevent kicks. The common reasons of cementation can be summarized as :

- Cement supports casing
- Ensures the isolation.
- Cemented casing provides a foundation for subsequent drilling
- Protecting the casing from corrosion.
- Preventing blowouts by forming a seal in the annulus.

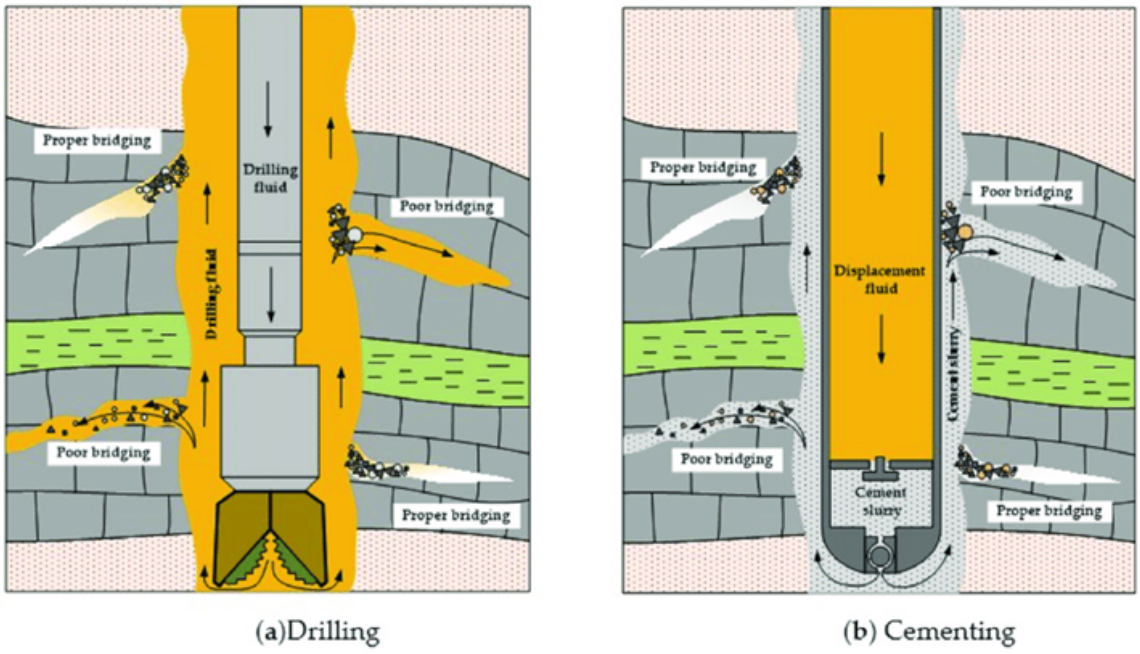

Figure I.1: Illustration of lost circulation during drilling and cementing

I.2.1 Axial Load

High axial loads can be imposed on the casing string and/or surrounding cement by landing and suspension methods and later operations. The cement strength required to support such axial casing loads can be determined through shear bond tests. Axial casing loads were found to be proportional to the area of contact between cement and the casing. Therefore, support coefficient, shear bond or sliding resistance, as it is described by various investigators, is the load required to break the bond, divided by the surface area between cement and pipe.

I.2.2 Zone Isolation

Although cement with low compressive strength may be adequate to handle axial and radial casing loads, high ultimate strength may be required for zone isolation. Zone isolation depends, in part, on load interactions between formation, cement and casing. Difficulty arises in determining type and magnitude of loads imposed by fluid pressure and drawdown and depletion of formations. For these reasons, only quantitative judgments

have been attempted, and these usually relate to the "hydraulic bond" which indicates adhesion between casing and cement, or between cement and formation.[2]

I.2.3 Corrosion

Corrosion in oil well casings poses a considerable challenge. It's primarily an electrochemical process, involving electrical currents between different metals. The presence of free water in the annulus acts as an electrolyte, its conductivity increasing with the levels of dissolved salts and metal ions. Moreover, gas in the wellbore, particularly in environments with hydrogen sulfide (H2S), can accelerate corrosion and induce embrittlement.

I.2.4 Blow out prevention

It's crucial to seal off the annulus for well control while drilling. Uneven cement setting can lead to bridging, diminishing the hydrostatic pressure on formations below. The quicker the cement sets initially or the longer it maintains full hydrostatic pressure during setting, the lower the likelihood of hydrocarbons or other fluids migrating through the cement. Such migration can result in severe issues, potentially leading to blowouts.

I.3 Primary cementing job

I.3.1 Definition

Primary cementing is the process of pumping a cement slurry in the annulus between the casing and the formation, it is called Primary because it’s the first attempt of pumping and it’s generally critical in determining whether the process is technically-economically succeeded or not. Because it’s the operation in which the success of drilling and completion is based on. It is usually one-shot-deal.

I.3.2 Secondary Cementation

In the other hand, there is remedial or secondary cementing, it comes to compensate the failure of the primary cementing. Therefore, a careful study and the perfect performance must be done because remedial cementing is costly and critical.

Squeeze cementing is the process of forcing a cement slurry through holes in the casing into the annulus. The primary objective in squeeze cementing is to develop a seal in the wellbore between formation intervals that during production tests have shown signs of detrimental communication. [3]

I.3.3 Primary cementing procedure

The main principle of primary cementing is to displace the cement slurry from its pumps to wellbore specifically in annulus between casing a well bore through the cement head to ensure the construction stability and consolidate the formation and prevent collapsing the well.

According to the casing type, there are many techniques largely used in primary cementing, including;

- Cementing through drill pipe (stinger): for large diameters, e.g. surface casing.
- Ordinary cementing: through cementing head and wiper plugs for most types of casing (intermediate casing, production casing).

Those techniques are mutual in most of the following sections except for pumping cement. Therefore, the distinction in the process will be detailed there.

I.3.3.1 Running casing

The drilling is stopped after achieving the desired depth and a logging unit confirms the geometry of the well by utilizing caliper tool in purpose of determining the accurate volume to be prepared.

A known dimension casing is run with centralizers and scratchers in exterior to keep it centered and clean the wall. except the conductor pipe (the first casing to be run), the casing is equipped with a guide show at its end and a float color to make a receptacle for cement plugs. A check valve assembly fixed within the float collar prevent drilling mud or cement slurry from entering the casing when pumping is halted.

Casing types

A. **Conductor pipe:** is the first casing to be run, it's relatively large (26" to 36") and short (3m to 30m).
Its main function is to guide the bit for to the correct position when start drilling and prevent the hole from caving in and washing out.

B. **Surface casing:** the next casing installed in a wellbore to protect groundwater from contamination, and isolate fresh water zones.

C. **Intermediate casing:** it is installed after surface casing and before intermediate casing to isolate abnormally pressured formations, lost circulation zones, salt sections.

D. **Production casing:** is the final casing to be run and cemented to surface, it isolates the production zone and provide a conduit for hydrocarbons to flow

E. **Liner:** is a suspended casing that does not extend to the surface, instead it hung in the previous casing. It provides flexibility for future operation such as stimulations thus it covers the last open hole.

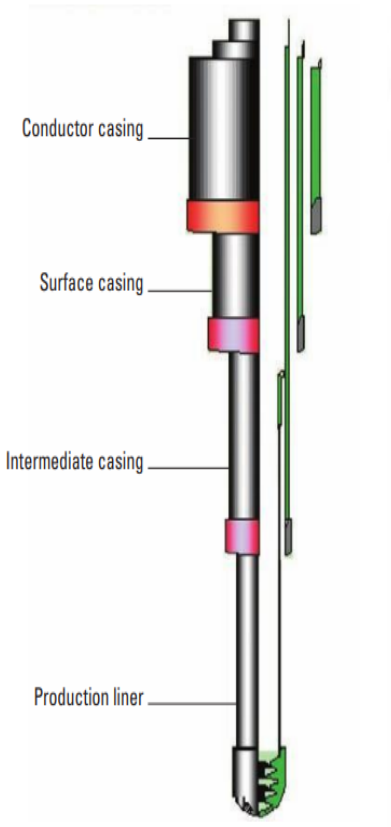

Figure I.2: Example of simple casing program

I.3.3.2 Conditioning the mud by circulating

A. Prior the casing:

Highly gelled mud and thick mud cake are formed during drilling unless a good mud conditioning is performed by increasing the circulating period prior to running the casing [1] It is therefore essential that mud properties are adjusted prior to reaching casing settling depth to obtain optimum parameters for running casing and cementing.

B. After the casing

After running casing, a mud circulation initiates and keep on as long as necessary to clear the well bore from debris and reduce bottom hole temperature and break up mud gels, some rotations during the casing running also benefits conditioning the mud in wellbore.

Drilling fluid parameters prevents leaks by building a sealing (mud cake) to the permeable formations. Maintaining this thin impermeable filter cake is also essential for the prevention of several possible problems, e.g., differential pressure sticking, logging difficulties, lost circulation problems and primary cementing problems. [2]

In the other hand, cement properties are not able to displace this gelled fluid unless it returns to its mobile state by circulating in different flow rates.

I.3.3.3 Pump spacer

Spacers are chemical liquids prepared to separate the drilling fluid phase and the cement slurry phase. They are designed according to several considerations includes; density, compatibility, viscosity, wettability…

The cleaning process is accomplished by bulk displacement following of the mud followed by cleaning of the annulus wall. Fluid mechanics and the rheology and density of the spacer or chemical wash ensure bulk displacement. [4] Its main function is to enhance the mud displacement and create an isolation between mud and cement slurry in order to prevent any chemical reactions and wet the formation by creating a reverse emulsion to the drilling fluid and make it conditioned for the cement to take place.

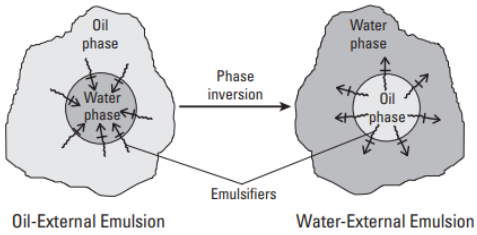

Figure I.3: Reverse the emulsion

I.3.3.4 Preparing slurry

A cement slurry is a mixture of water, Portland cement, and additives. Its formulation is designed in the laboratory to ensure some characterizations by utilizing special additives such as: accelerators, retarders, extenders, weighting agents and dispersants.

Each of the previous compositions give a desirable property to the cement slurry, before aligning the path to wellbore through cement head, laboratory tests should be done.

1. **Mixability**: mixing the water, additives and cement by using a mixing devise (blender) according to API specifications.
2. **Density:** it is a measurement of fluid weight per unit of volume.
   In the selection of slurry densities, factors beyond just pore and fracture pressures often come into play. In the same allowed interval, it may not accept densities lower than spacers.
   the density should be at least 10% higher than spacer's density.
3. **Rheology:** typical rotational viscometer is used to measure the rheological properties and characterizes the rheological behavior of fluids used in well cementing. 10sec and 10 min static gels are also taken by using viscometer**.**

Figure I.4: Viscometer

4. **Free fluid**: it determines a slurry's capacity to prevent fluid separation in static condition. Both during placement and after it has been placed into wellbore. A graduated glass cylinder and a free fluid test devise is used to measure the % of free fluid of a slurry**.**

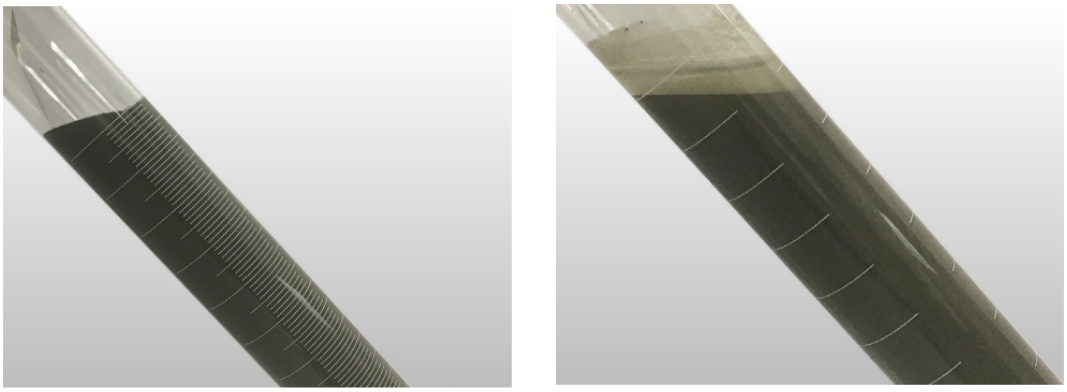

Figure I.5: Free water separation phenomenon

5. **Fluid loss:** it determines the effectiveness of a cement slurry composition in preventing the loss of water from the slurry to a formation in the wellbore. The stirring fluid loss tests and static fluid loss tests are commonly performed to determine the fluid loss of a cement slurry.

Figure I.6: Consistometers

6. **Thickening time;** determines the length of time a slurry will remain pumpable under simulated well conditions. The T.T test can simulate temperature, pressure, and time. Some retarders may be applied if there is a high temperature gradient in a given well, adding silica flour is one of the most solutions for this issue. Otherwise, a pump failure will occur, and real consequences will damage the process.

   This test is assured by using a special device called consistometer, which measures the consistency of the test slurry contained in a rotating cup while under simulated wellbore conditions.

Figure I.7: Fluid loss test

7. **Compressive strength** it determines the strength of a cement composition under temperature conditions simulating well conditions. Crush compressive strength and ultra-sonic strength are performed to estimate the compressive strength of cement slurries. This C.S is performed at BHST.

8. **Compatibility**; engineers assess the compatibility of the cement slurry with drilling fluids, formation fluids, and any other fluids present in the wellbore to prevent contamination, fluid loss, or unwanted reactions. It is performed to determine the degree of compatibility of wellbore fluids in cementing operations and includes the examination of rheological properties.

   Gel strength, thickening time, compressive strength, solids suspension, and spacer surfactant screening. By performing this test incompatibility tendencies can be determined and the selection of proper preflushes and/or spacers can be made.

No.	Ratio Mud or Cement Slurry to Spacer (vol. %)	Mixing Scheme
1	95/5	380 ml mud or cement slurry/20 ml spacer
2	75/25	300 ml mix **No.1** plus 80 ml of spacer
3	5/95	20 ml mud or cement slurry/380 ml spacer
4	25/75	80 ml mud or cement slurry plus 300 ml of mix **No.3**
5	50/50	Equal parts (200 ml) of mix **No.2** and mix **No.4**
6	25/50/25 mud/spacer/cement	Equal parts of mix **No.5** mud/spacer and mix **No.5** cement slurry/spacer

Table I.1: Mixture of testing

I.3.3.5 Pump cement slurry

A. Through cement head

After installing cement head and pumping spacer, bottom wiper plug is then release from the bottom valve as shown in **Figure I.8**. Wiper plugs give the advantage of separate drilling mud and spacer and cleaning casing internal walls it is used especially if there is a high differential in fluid densities to prevent contamination of mud and spacer and cement slurry and prevent intermixing of these fluids. Then we start pumping the prepared volume of slurry with a precalculated flow rate, once reaching sufficient volume we stop pumping and putting a superior plug. To increase pressure, another volume of mud should be pumped for the displacement until lower plug is placed in its seating then we regard pressure until the two plugs are contacted together then the pressure would increase abnormally.

B. Cementing through drill pipe stinger

An alternative method for cementing large diameter casing uses drill pipe for pumping cement slurry to the bottom. Cementing through drill pipe is accomplished by sealing a drill pipe stinger sub in a special cementing collar with a drillable sealing receptacle. There are some advantages in this method. It features low internal pressure, better displacement control and time savings in the cementing job because less mud has to be displaced. [5]

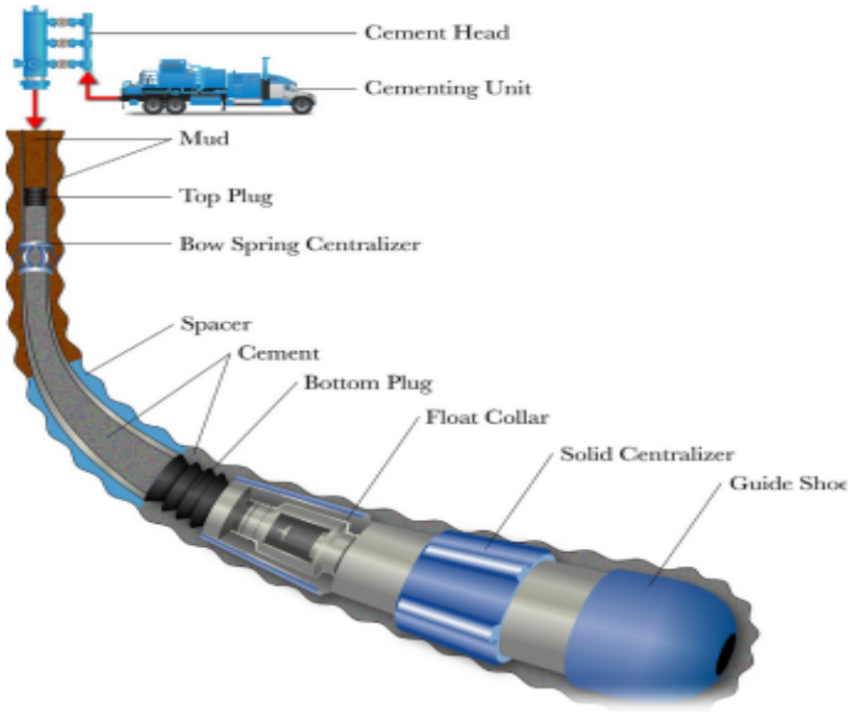

Figure I.8: Illustration of primary cementing equipments

I.3.3.6 Wait on cement

This period, ranging from a few hours to several days, is for liquid cement slurries to solidify and develop sufficient compressive strength. Meanwhile, pipe-cement and formation-cement bonds begin to develop, ensuring the ultimate goal of zonal isolation. [5]

I.3.3.7 Evaluate cement job

After the cement is set, we want to confirm that the cement is in place to provide the desired performance. The first indication that the cement is in place is when cement job measurements

including fluid volumes, cement density, surface pressure, and returns all match pre-job expectations. If there are any concerns with the top of cement (TOC), cement quality, or if it is required, a temperature survey or cement evaluation log should be run. A temperature survey, run several hours after cement placement, takes advantage of the heat generated by the cement column in the annulus. It is very useful to determine the location of TOC.

Cement bond log (CBL) is obtained using acoustic waves sent by a transmitter and received by a receiver. The variation of the acoustic wave amplitude represents the quality of the cement bond. Variable-density log.

(VDL) is another method to evaluate the quality of a cement job, which presents the amplitude of acoustic waves in various shades of a greyscale to identify the cement bond quality. One of the purposes of the casing and cementing is to provide a solid foundation for subsequent drilling operations. To ensure the quality of a cementing job, it is common to pressurize inside the newly cemented casing until the pressure at the shoe reaches the maximum anticipated pressure at that depth during the next drilling operation. If the pressure declines significantly or if there are other indications of leakage, the casing should be recemented using squeeze cementing operation. CBL and VDL tests are implemented to know if we have a good cement and guarantee that there is no risk to continue drilling unless we utilize other operations such as squeeze cement [5]

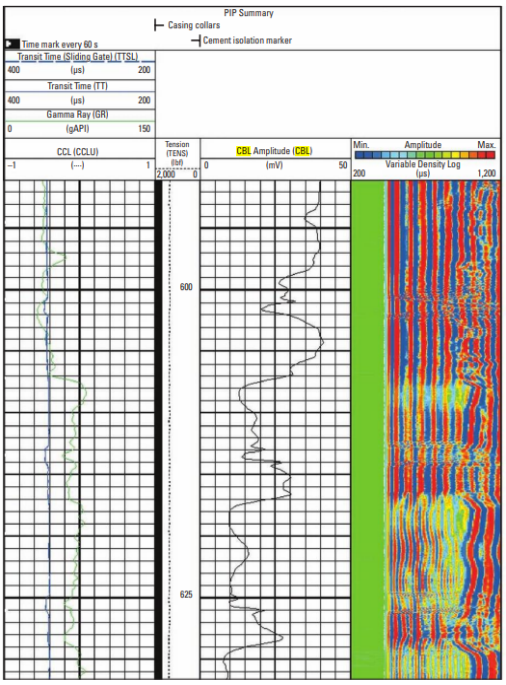

Figure I.9: Cement bond log

I.3.4 Challenges in primary cementing job

Practical part of the cement job is quite different than the theorical one, exterior factors will present a difficult not predicted changes in the process, and rapid decisions should be adopted. Some common challenges include; gas flow, zonal communication, pump pressure, poor mud removal.

I.3.4.1 Gas flow

Since the purpose of cementing is to ensure zonal isolation and prevent fluid communication, just a simple mistake in executing the process can fail the aim.
Gas flow is a phenomenon occur in productive zones when the likelihood of some gas kicks are presented, if the integrity of the slurry is weak some channels will allow the gas to migrate and create a major problem which is cracks full of gas bubbles in annulus. This issue increases the annulus pressure and lead to further risks such as blow out.

I.3.4.2 Zonal communication

Bad mud removal is a part of many issues such as zonal communication that makes path for fluids to flow from layer to layer.
Zonal communication weakens the well integrity (risk of collapsing the well), and threatens the environment (contamination of fresh water, dissolution of salt formations…).

I.3.4.3 Pump pressure

Pump pressure effects on both bottom hole pressure **BHP** and flow regime. Higher pump pressure can help ensure proper placement of cement, enhancing well integrity. However, excessive pressure can lead to formation damage or even fracturing. Controlling pump pressure is crucial for maintaining the desired flow regime and BHP through the assistance of computer simulator, and with careful study in rheological models and fluid properties a convenient pump pressure can be selected. Consequences of bad pump selection are:

A. Lost circulation

Lost circulation is a result of fracking the weak matrix of the formations, it may occur when running the casing and/or when cementing. It is the reason why most cement volume calculations cannot cover all the annulus. Environmental issues also are another consequence of this problem. Cement slurries are heavier than drilling fluids, this difference of density creates much pressure which will be applied on bottom hole formation and the risk of exceeding the frac pressure of matrix may exist. Therefore, dynamic pressure is the key to manipulate downhole total pressure the less pump pressure the less stress applied on bottom hole formations.

B. Lifted casing

A good centralization of casing is not enough to have a good cement bond, because an excessive pressure in casing shoe can increase the effect of buoyancy force and move the casing upward. Lifting casing from its depth is a remarkable issue affect the hole process and cost more expenses. Reducing pump rate is a solution for that problem, also a good fixing on top of wellhead can prevent this risk.

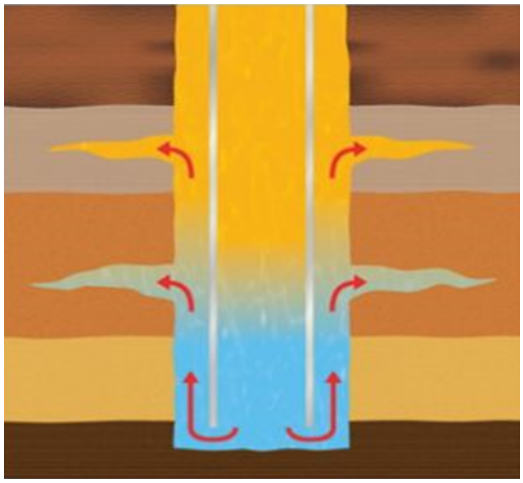

Figure I.10: Lost circulation

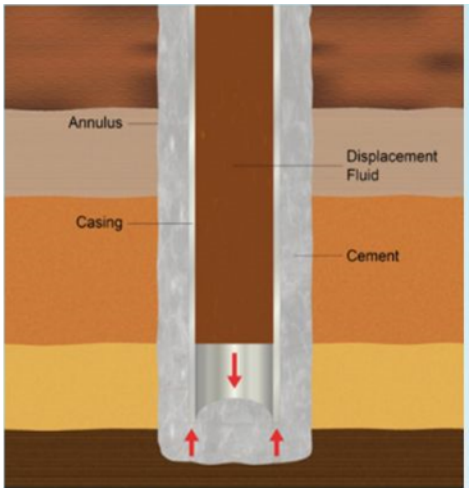

Figure I.11: Lifted casing

I.3.4.4 Poor mud removal (displacement efficiency)

Displacement efficiency is a complex subject to take care of when designing the cement job, The wiper plugs and the spacer are essential for maintaining the path clear for cement slurry, but sometimes this goal cannot be achieved due bad mud removal.

Muds and slurries are incompatible fluids, when they mixed a viscous layer will be created and it is difficult to displace. [6]

Displacement efficiency is affected by different forms of mud existing in the wellbore, as depicted in **Figure I.12**, including moving mud, gelled mud, and mud cakes. Under high pressure, mud is forced against the formation, and liquid component is filtered through the formation, while a hard layer is left sticking on the wall. Chemical washes can be used to clear mud cakes. Next to the mud cake, a static gelled mud layer may exist, when viscous shear stress is not high enough to mobilize it.

Mud is a non-Newtonian fluid that has the property of gelling in static, because of that the mud column will be divided in parties. [6]

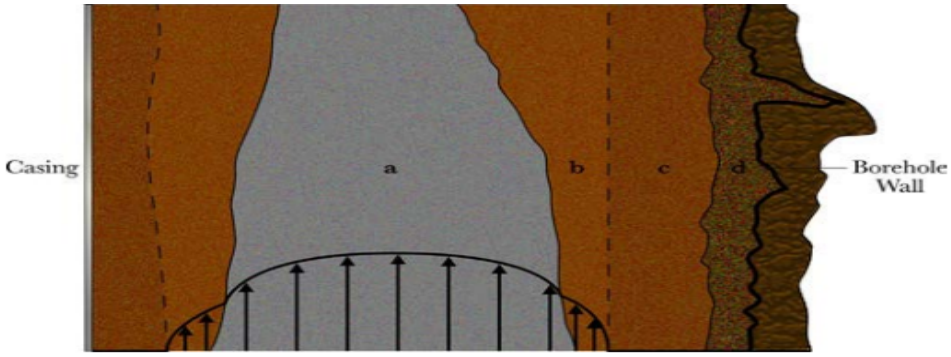

Figure I.12: Illustration of different forms of mud existing near the formation and casing inside the well.

In the figure, the letters **a, b, c,** and **d** represent displacing fluid, flowing mud, gelled mud, and mud cake, respectively. (Credit: Pegasus Vertex, Inc).

4.2. Poor centralization:

Running down the casing usually equipped by centralizers and scratchers that keeps it in the center of the wellbore, this consideration has not to be neglected because cement slurry flows in the easiest path therefore an equal annular space between the hole walls and outside the casing have to be respected.

All the common cementing challenges can be explained in the following table:

Factor	Effect on Bond Log
Micro-annulus	A small gap between the cement and pipe (e.g. from the casing OD shrinking with reduced wellbore pressure) can lower the attenuation of the casing arrival and hinder the wave propagation across the gap. The result is a pessimistic interpretation, mistaking the microannulus for “no cement in the annulus at all”. Running the log with pressure applied inside the pipe to close the microannulus will compensate for this effect.
Fast formations	Formations that transmit a sonic signal faster than the steel in the casing. The result on a CBL/VDL is, that instead of evaluating the casing arrival and its attenuation, the tool evaluates the arrival signal from the fast formation, which is generally not much attenuated. The result is an inaccurate lowquality interpretation of the cement bond.
Uncured cement	Induced vibrations dissipate in a liquid slurry, appearing on the log similar to the drilling fluid or spacer. This leads to a “false” interpretation that the presence and/or quality of a given cement job is lower than it actually is.
Lightweight (or foam) cement	Low density cements exhibit a lower impedance and generally lower attenuation, even if fully bonded. For CBL/VDL Logs, this can lead to a higher 100% bond amplitude. For impedance-based logs, this can lead to a misinterpretation, if the log looks for set cement in the wrong impedance window. This can lead to a “false” interpretation that the presence and/or quality of a given cement job is lower than it actually is. Applying pressure has no effect on the evaluation.
Thick walled pipe	The thicker the pipe, the lower the amplitude of the free pipe is. This reduces the sensitivity of a sonic log and impedes the signal strength of an ultrasonic log signal. The result is that, even in a zonally isolated interval, the bond log may show poor results. Logging tools generally specify a maximum wall thickness through which their results are considered valid.

Heavy wellbore fluid	Heavy wellbore fluids hinder the propagation of sonic and ultrasonic signals. Logging tools are generally rated for a range of logging fluid densities, beyond which their response becomes unreliable. Pad tools, which directly connect to the tubular wall can avoid this problem.
Thin cement sheath	Cement sheaths less than ¾ inch thick will not result in full attenuation, meaning that even well bonded cement may show poor results.
Tool eccentricity	Poor eccentricity can seriously affect the results of acoustic logs by artificially reducing the amplitude, which in turn can indicate annular cement fill when in fact the casing is totally unsupported. Causes for tool eccentricity include improper equipment (incorrect size or broken centralizers), weak centralization in deviated wells, damaged or bent tool housing, or damaged casing.
Mill scale and other suspended particles	Can lead to “false” readings and interpretation that the presence and/or quality of a given cement job is lower than it actually is.
Improper setting of “gates” on the first arrival of signal	The “gate” is the time interval after an acoustic signal is sent, in which the tool is looking for the arrival of the signal. If the gate is set wrongly, the tool will evaluate a wrong signal or a wrong part of the signal, rendering the log result inaccurate and irrelevant.
Improper or no calibration of the tool	Sonic tools require a calibration to the signal of free, uncemented pipe. Other tools require calibration to the fluid the log is taken in and other well parameters, as well as correct setup of the impedances the tool interprets as solid, liquid or gaseous.. Ensure the tool is not straddling a collar when calibrating for free pipe, and the depth at which the tool was calibrated should be noted on the log header. Similarly, all other settings and calibration factors [should be listed in the log header. [7]

Table 1.1: Factors effecting on cement bond logs from Halliburton rapport

CHAPTER II

GENERALITIES ON SLURRIES RIOLOGY

II.1 Fluid Dynamics Overview

This chapter delineates the categorization of fluids and delineates between Newtonian and non-Newtonian fluid dynamics. We briefly explore the microstructure of non-Newtonian fluids and its impact on the rheological characteristics of fluids. Rheology, its definition, and the varied perspectives within literature regarding rheological characterization exploring the different models used in most studies of the field and with model selection are outlined, thorough grasp of the rheological properties of cement slurries is crucial for the design and assessment of a successful primary cementing operation. Proper rheological characterization is vital to:

- Assess the mixability and pumpability of the slurry.
- Enhance mud removal and ensure effective slurry placement.
- Calculate the friction pressure as the slurry flows through pipes and annular spaces.
- Determine the slurry's capability to transport large particles, such as certain lost circulation materials and fibers.
- Forecast the impact of the wellbore temperature profile on slurry placement.
- Predict the annular pressure following slurry placement.

II.2 Rheology Definition

Rheology is the science of deformation of material. The name was coined by Eugene Bingham, who founded the Society of Rheology in the USA, and its root lies in the Greek word for flow [8]. It includes the theory ‘underlying’ the deformation and the practice of measurement by the study of the flow of matter, primarily in a liquid state, but also as soft solids or solids under conditions in which they respond with plastic flow rather than deforming elastically in response to an applied force. So, It is a branch of physics that deals with the deformation and flow of materials, both solids and liquids. Rheology is particularly concerned with the properties of fluids that affect their ability to flow, including viscosity, which is a measure of the relationship between flow rate (shear rate) and the pressure gradient (shear stress) that drives fluid movement.

Rheology has a wide range of applications across various fields such as materials science, engineering, geophysics, physiology, human biology, and pharmaceutics. In materials science, it is critical for producing substances with intricate flow properties, such as cement, paint, and chocolate. Furthermore, the theory of plasticity plays a vital role in designing metal forming processes. Rheology is essential in the production and application of polymeric materials, impacting numerous products in the industrial and military sectors due to the characterization of viscoelastic properties. In pharmacology, understanding the flow properties of liquids is crucial for manufacturing various dosage forms, including liquids, ointments, creams, and pastes. The

study of how liquids behave under stress is particularly important, with flow properties serving as crucial quality control measures to ensure product consistency and minimize variations between batches.

II.3 Classification Of Fluids

Rheology," originally centered on the study of material deformation, places significant emphasis on viscosity as the primary factor influencing this phenomenon. Viscosity serves as a measure of a fluid's resistance to deformation at a given rate, known as the intuitive notion of "thickness" in liquids. Scientifically, viscosity is defined as the product of force, time, and area, with its SI units expressed as newton-seconds per square meter, or pascal-seconds[9] . To determine a fluid viscosity value, one collects data from a Fann meter for a small sample of slurries, post-processes the data using a fluid model. A fluid can be treated as Newtonian, such as water, or non-Newtonian depending on real-life conditions. A difference between Newtonian and non-Newtonian fluids is determined based on the relationship between the shear stress to the shear strain rate. A Newtonian fluid has a linear relation of the shear stress to the shear strain rate and requires no initial stress to begin fluid motion. A non- Newtonian fluid is simply any fluid that behaves in a way contrary to Newtonian behavior.

The rheological properties of suspensions are often related to a vaguely defined property referred to as structure. "There is a direct and strong link between the type and extent of non-Newtonian flow behavior on the one hand, and the response of the structure to externally applied forces on the other" [10]

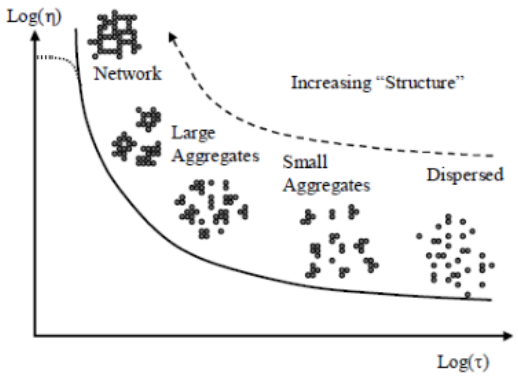

Figure II.1: The effect of viscous shear stress on particle structure (Hallbom, 2008)

Casson (1959) described structure to be the formation of chains of needle-like ink particles causing an increase in apparent viscosity in much the same way that increasing molecular weight causes an increase in viscosity in polymers. Scott Blair (1967) defined the degree of structure of a slurry as being a function of the number of formed bonds between particles per unit volume,

thus a higher bond density would cause a higher apparent viscosity. Hallbom (2008), successfully developed the most recent rheological model for shear-thinning slurries, and based his work on the theory that at higher shear rates the structure breaks down and particles become fully dispersed enabling the average particle bond strength to increase. He thus defines structure as a property which is related to the average size of the aggregates, which generally decreases as the shear rate increases. This phenomenon is illustrated (**Figure II.1**).

Rheological models of time-independent fluids

Fluids are commonly categorized based on their response to externally applied pressure (i.e., shear stress) or the resultant effects under applied shear rates [10]. Metzner (1956) proposed a classification for non-Newtonian fluids into three main categories:

1. viscoelastic fluids, where stress recovery occurs post shear deformation,
2. time-dependent fluids, where shear stress-shear rate relations are contingent on the duration of shear application, and
3. time-independent fluids, where shear-stress shear rate relations remain unaffected by the duration of shear application. Time-independent fluids are further subcategorized into shear thinning and shear thickening fluids[11]. For this study, only time-independent shear-thinning fluids were under consideration.

When this group of fluids is characterized by viscosity relations that are a function of shear rate, but not of time application of shear, the rheological behavior of these fluids is described by governing relations (constitutive equations), between shear stress τ and shear rate γ. Models of non-Newtonian fluids can be categorized as Power Law, Bingham Plastic, or Herschel-Bulkley[9] . Many other non-Newtonian models exist, but for the purpose of engineering applications only some of the simpler models with only two or three model parameters are considered in this study (The three above). The complexity of the other models caused they gained less popularity in the industry.

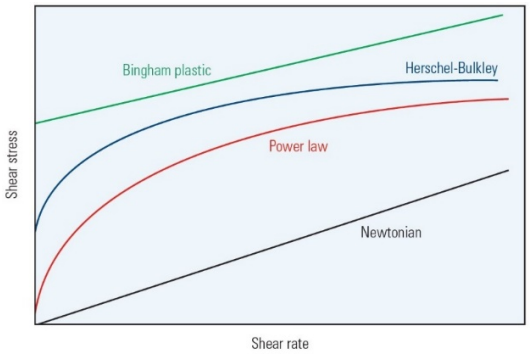

Figure II.2: Stress/Shear rate curve for fluids (Schlumberger site).

II.3.1 Newtonian Fluids

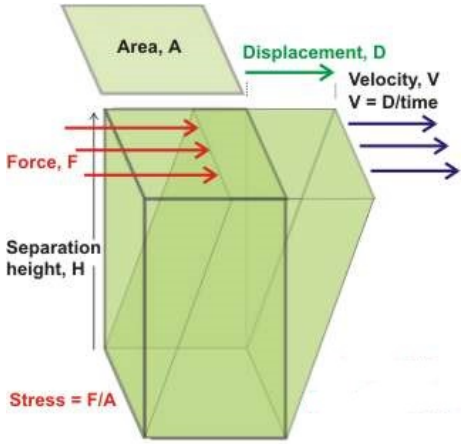

Figure II.3: A sketch for simple shear deformation

Consider a slender fluid layer positioned between parallel plates, as depicted in **Figure II.3**, with a distance (H) between them. Under steady-state conditions, the fluid experiences shearing due to the application of force (F), countered by an opposing force of internal friction within the fluid. To qualify as an incompressible Newtonian fluid under laminar flow, the shear stress τ must be proportional to the product of the shear rate (γ) and the fluid's viscosity. The shear rate is described as the velocity gradient (V) perpendicular to the direction of the applied shear force.

$$\frac{F}{A} = \tau \qquad .(2.1) \qquad\qquad \tau = \mu \times \gamma \quad .(2.2)$$

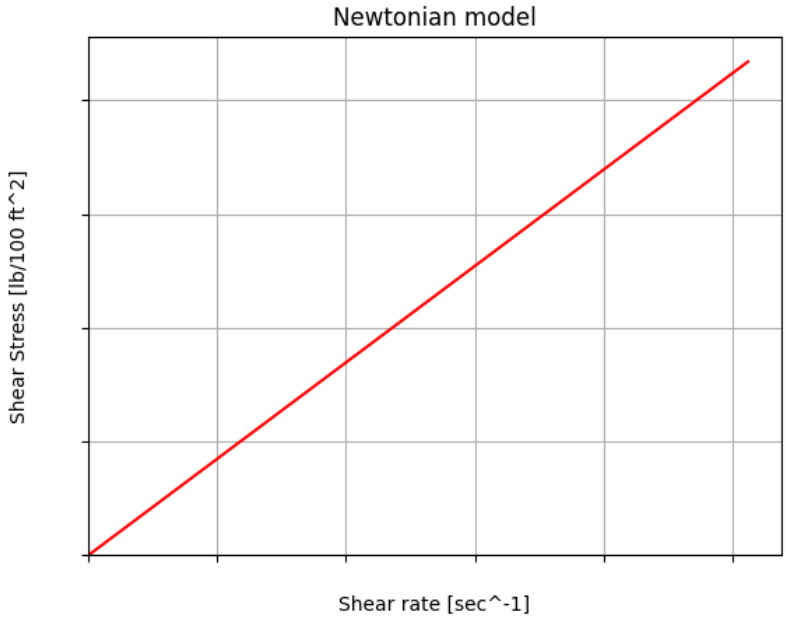

Figure II.4: Rheogram for Newtonian fluid

The ratio of the shear stress to the shear rate is called the Newtonian viscosity μ. It is independent of shear rate γ or shear stress τ and depends only on the material at given temperature and pressure. A plot of shear stress τ and shear rate γ called the "flow curve" or rheogram, for a Newtonian fluid is therefore a straight line with a slope μ passing through the origin. The single constant completely characterizes the flow behavior of a Newtonian fluid at a fixed temperature and pressure.

II.3.2 Bingham Plastic Model

As originally presented by Bingham in 1922, The Bingham plastic model was the first two-parameter model with the simplest constitutive equation describing the flow behavior of a yield stress fluid in one-dimensional that gained widespread acceptance in the drilling industry and is simple to visualize.

As shown in **Figure II.5**, the distinguishing characteristic of a Bingham plastic fluid is that it will remain unsheared until the applied stress reaches a minimum value to initiate flow (unlike the Newtonian fluids) and then have a linear dependence of the shear strain rate to shear stress.. Two parameters define the Bingham plastic model:

- The value of τ for γ = 0 is τ_y
- The slope of the straight line, μ_p

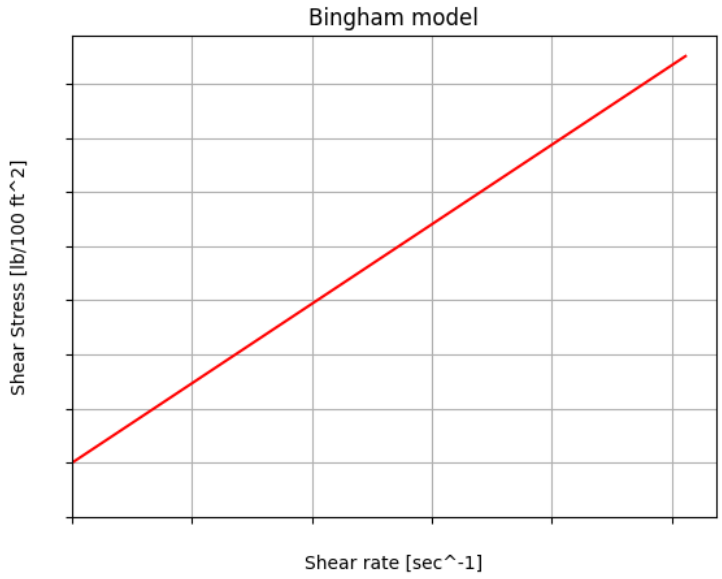

Figure II.5: Rheogram for Bingham plastic model

Bingham fluids behave in a manner described by the following equations:

$$\tau = \tau_y + \mu_p \times \gamma \quad .(2.3)$$

- μ_p is constant and is called the plastic viscosity.
- τ_y is called the Bingham yield stress.

The Bingham parameters, yield point τ_y and plastic viscosity μ_p can be estimated from the graph, which can be drawing with curve fitting using linear regression or can be calculated by the following **equations (2.4)** and **(2.5)**

$$\mu_p = \theta_{600} - \theta_{300} \quad .(2.4)$$

$$\tau_y = \theta_{300} - \mu_p \quad .(2.5)$$

However, the Bingham plastic model does not accurately represent the behavior of drilling fluid at very low shear rate in the annulus and at very high shear rate at the bit[12] hence, a modification of the model in terms of introducing stress correction factor is not only necessary but of utmost importance. This is because accurate determination of drilling fluid rheological parameters is important for the following applications, calculating frictional pressure loss in annuli and pipe, estimating Equivalent Circulating Density (ECD) of the fluid under downhole conditions, determination of flow regimes in the annulus, estimation of hole-cleaning efficiency, estimating surge and swab pressures and optimization of the circulating system for improved drilling efficiency**.** The yield strength τ_y is the true shear stress at zero shear-rate and relates to the state of flocculation of the drilling fluid at rest. It is more representative of the structure formed at rest than the yield point value. And its value is usually approximated by measuring the shear stress at 3 RPM.

II.3.3 Power Law Model

The Bingham plastic model assumes a linear relationship between shear stress and shear rate. However, a better representation of the behavior of a drilling fluid is to consider a Power-law relationship between viscosity and shear rate in such the apparent viscosity decreases with an increase in shear rate. Within Power Law fluids there are fluids whose viscosity increases with the rate of shear and those with viscosity that decreases with the rate of shear. These are called 'shear thickening' or dilatant and 'shear thinning' or pseudo-plastic fluids, respectively[9] . Rarely do non-Newtonian fluids behave exactly according to either of these two models. This is termed shear-thinning rheological behavior and is described by the power-law model, given by **Equation 2.6**

$$\tau = K \times \gamma^n \quad .(2.6)$$

The power law model, also known as the Ostwald de Waele relationship, is used to fit non-Newtonian data across shear rates where there is no evidence of a Newtonian plateau region. Fitting to the power law model is appropriate where the measured data is entirely within the shear-thinning regime across all the shear rates tested. The power law model only has two fitting constants making it much simpler than other models that fit non-Newtonian fluids such as the Cross model or Carreau-Yasuda model which contain four and five fitting constants, respectively.

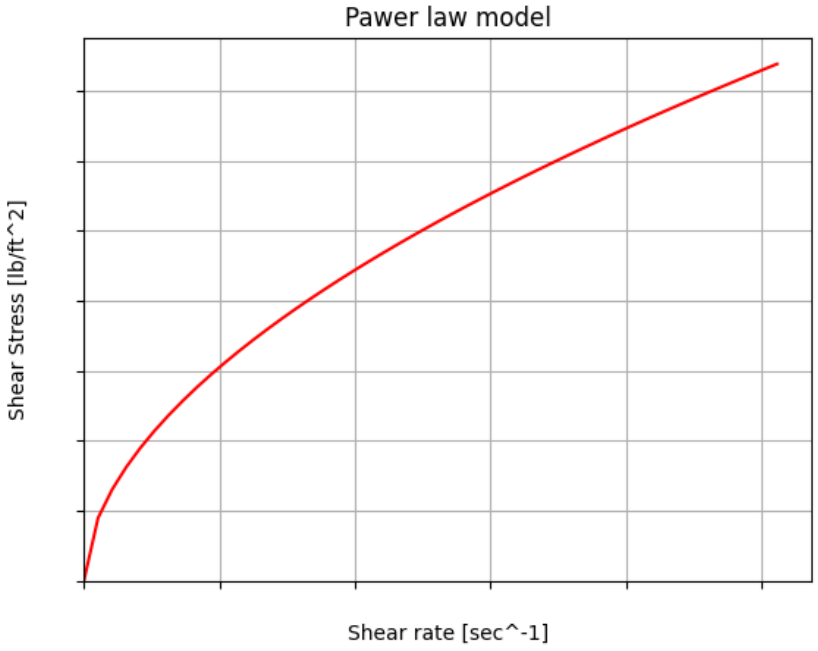

Figure II.6: Rheogram for Power law model

Equation 2.6 can be linearized as follows:

$$\log \tau = \log K + n \times \log \gamma \qquad .(2.7)$$

where n is determined from the slope of the curve fitting line and K is the exponential of the y intercept $\log K$.

Note that the estimations of Power-law parameters can be made also by the following equations:

$$n = 3.32 \times \log\frac{\theta_{600}}{\theta_{300}} \quad .(2.8)$$

$$K = 510 \times \frac{\theta_{600}}{511^{n}} \quad .(2.9)$$

The variables K and n are curve fitting parameters known as the fluid consistency index K and the flow behavior index n. Shear-thinning behavior occurs for $n < 1$. Fluids that behave this way are also called pseudoplastic fluids. As the value of n decreases, the degree of shear thinning increases. For $n > 1$ shear thickening occurs and such fluids are called dilatant fluids.

When $n = 1$, the model reduces to **Equation 2.2**

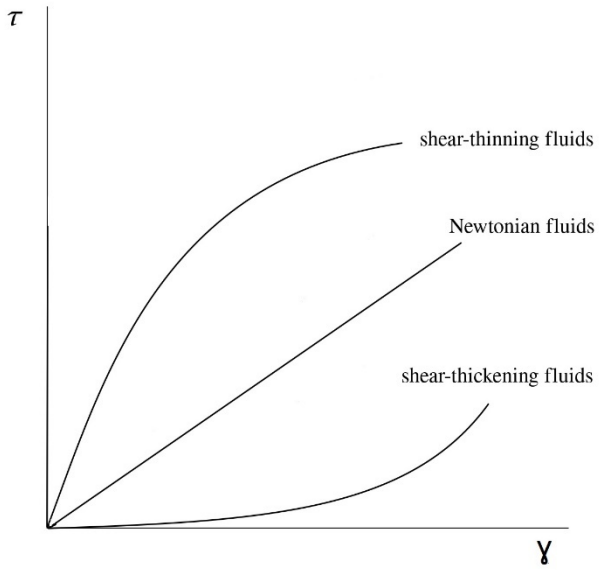

Figure II.7: Shear thinning and shear thickening rheogram differences

Shear thinning fluid behavior is advantageous in the oil and gas industry, particularly during drilling operations where drilling muds display shear-thinning properties. These drilling muds, such as bentonite slurry, must be thin enough to pump easily yet viscous enough to carry cuttings to the surface. In contrast, shear thickening behavior can sometimes be problematic in the oil and gas industry, as it can cause equipment and operational issues when the fluid suddenly becomes harder to pump. Nonetheless, certain drilling fluid additives, such as polymer-based additives used to control fluid loss and enhance wellbore stability, can exhibit shear-thickening properties. Understanding these behaviors is crucial for selecting and managing fluids to optimize performance and efficiency in various processes.

Generally, the power-law model applies only over a limited range of shear rates, and the fitted values of K and n depend on the range of shear rates considered. The value for K also depends on the value for n, thus K values cannot be compared for varying values of n. The Power-law model provides more information in the low-shear-rate condition but still has a weakness at high shear rates.

II.3.4 Herschel-Bulkley model

Most often fluids exhibit some characteristics of both Power Law and Bingham Plastic fluids. The blend of these two models is the Herschel-Bulkley model. Fluids that obey this model are called Plastic fluids[13] . The Herschel-Bulkley model was first proposed by Winslow Herschel and Ronald Bulkley in an article published in 1926.

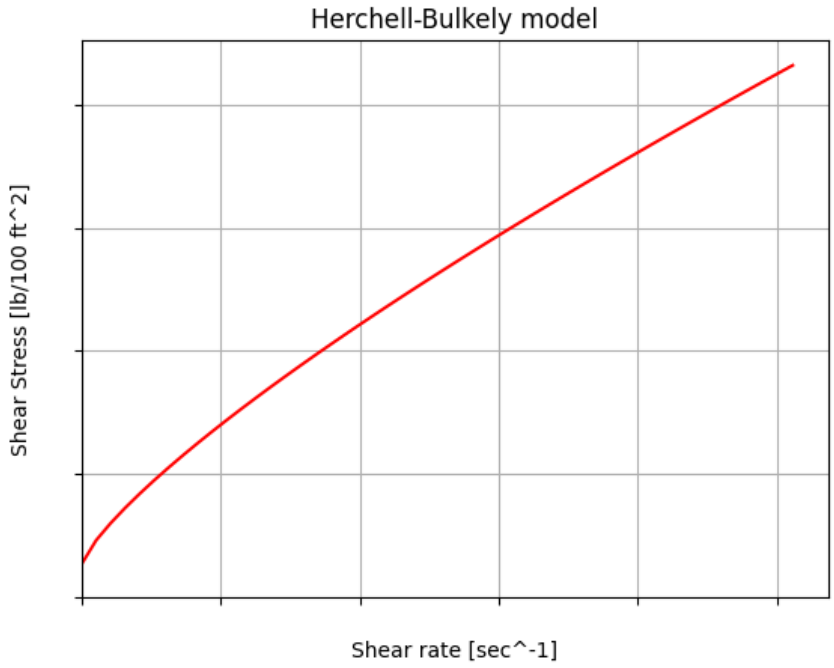

Figure II.8: Rheogram for HB model

And its curve is illustrates a nonlinear relationship between the shear rate and shear stress with a nonzero shear stress value at zero shear rate. An initial force is required to deform and mobilize the fluid. The flow resistance increases less-than-linearly with deformation. The flow behavior of the Herschel and Bulkley fluids is described by the Herschel and Bulkley model expressed as

$$\tau = \tau_0 + K \times \gamma^n \qquad .(2.10)$$

The Herschel-Bulkley model is commonly used to describe materials such as concrete, mud, dough, and toothpaste, for which a constant viscosity after a critical shear stress is a reasonable assumption when a log-log graph is made. In addition to the transition behavior between a flow and no-flow regime, the Herschel-Bulkley model can also exhibit a shear-thinning or shear thickening behavior depending on the value of n. In the most common case, in which n is smaller than 1, Herschel-Bulkley fluids are shear thinning. Their viscosities vary from infinity at 0 shear rate to 0 at infinite shear rate. As with power-law fluids, this lower limit is not physically sound, and caution should be exercised when applying this three-parameter model to situations outside the shear-rate range in which the rheological characterization was performed. Obviously, this three-parameter model is a general model that can be used to describe the behavior of all fluids. The Herschel-Bulkley model is widely used by office engineers in designing fluid hydraulics.

Equation 2.10 can be linearized as follows:

$$\log(\tau - \tau_0) = \log K + n \times \log \gamma \qquad .(2.11)$$

Here, we use $\mathbf{\log(x+1)}$ to transform the rotational speed and the average of dial reading to achieve a more gradual decrease in slope, resulting in a more curved flow curve.

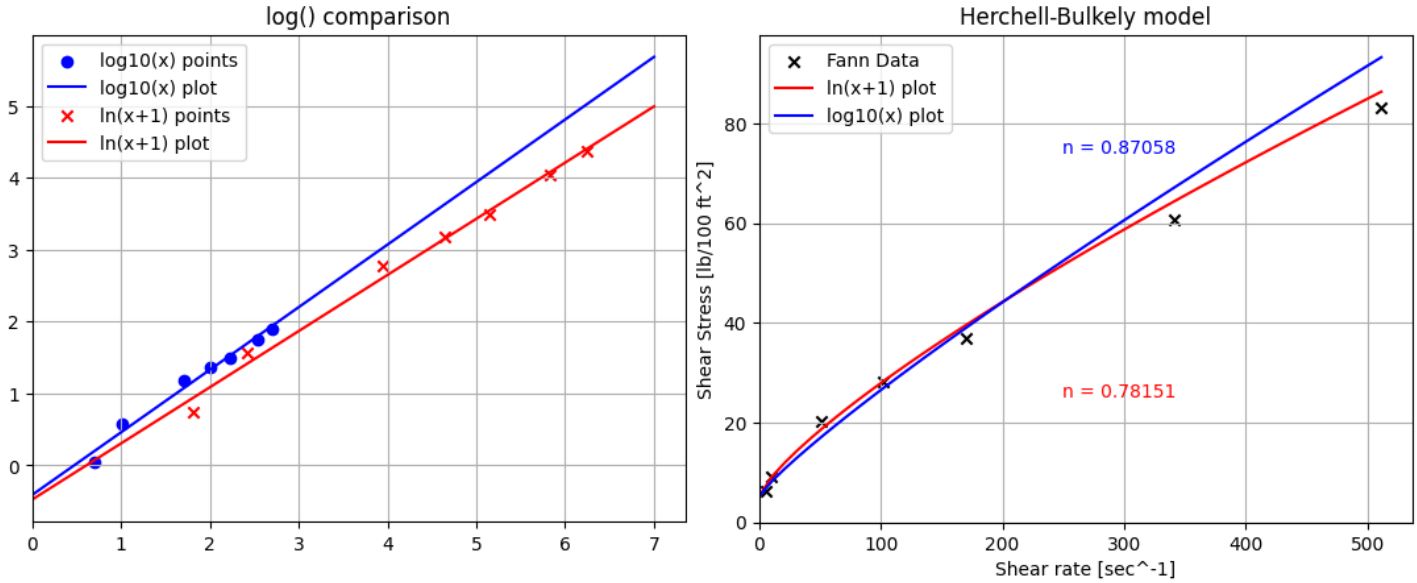

Figure II.9: Comparison between use of $\log(x)$& $\log(x+1)$ functions.

Since this is a three-parameter model, an initial calculation τ_0 is required for other parameter calculations. τ_0 is calculated by Versan and Tolga.

$$\tau_0 = \frac{\tau^{*2} - \tau_{min} \times \tau_{max}}{2 \times \tau^* - \tau_{min} - \tau_{max}} \quad .(2.12)$$

where $\tau^*$is the shear stress value corresponding to the geometric mean of the shear rate γ^*

$$\gamma^* = \sqrt{\gamma_{min} \times \gamma_{max}} \quad .(2.13)$$

Then using this value γ^* we can interpolate between values of shear stress obtained from FANN viscosity meter reading. The Herschel-Bulkley equation is preferred to Power-law or Bingham relationships because it results in more accurate models of rheological behavior when adequate experimental data are available. The yield stress is normally taken as the 3 RPM reading. However, we are taking Versan and Tolga's approach to obtain τ_0. Then n and k values can be calculated from the 600 and 300 RPM values or graphically with the curve fitting line log-log graph.

- **Unified Model**

The Unified model is an improved version of a simplified Herschel-Bulkley model established by the drilling industry. See **Equations 2.4 and 2.5**. The calculations of rheological parameters for the Unified model n and k involve previous estimation of plastic viscosity μ_p, yield point τ_y, and yield stress τ_0. See **Equations 2.7 and 2.8** for estimation of plastic viscosity and yield point respectively.

To estimate τ_0 for the Unified model, Zamora and Power give the following alternative:

Take low shear yield point τ_{yl} as τ_0. This is calculated from **Equation 2.14**.

$$\tau_{yl} = (2\theta_3 - \theta_6) \times 1.067 \quad .(2.14)$$

Where:

- τ_{yl} is lower shear yield point.

The equations proposed for this model to estimate n_p and n_a, and K_p and K_a are the following

Pipe Flow:

$$n_p = 3.32 \times \log \frac{2 \times \mu_p - \tau_y}{\mu_p - \tau_y} \quad .(2.15)$$

$$K_p = 1.066 \times \frac{\mu_p - \tau_y}{511^{n_p}} \quad .(2.16)$$

Annular Flow:

$$n_a = 3.32 \times \log \frac{2\times \mu_p - \tau_y - \tau_0}{\mu_p - \tau_y - \tau_0} \qquad .(2.17)$$

$$K_a = 1.066 \times \frac{\mu_p - \tau_y - \tau_0}{511^{n_a}} \qquad .(2.18)$$

II.4 Flow regimes

Flow regimes commonly encountered in well cementing include laminar flow, turbulent flow, and transitional flow. In laminar flow, the fluid moves as parallel layers at a uniform or nearly uniform velocity, with no large-scale movement of particles between layers. The fluid layers near the center of the pipe or annulus move faster than those near the casing wall or well bore. Turbulent flow, on the other hand, is characterized by velocity fluctuations among fluid particles both parallel and perpendicular to the mean flow, resulting in a chaotic flow pattern. Transitional flow exhibits features of both laminar and turbulent regimes, representing the difficult-to-define region where flow is neither completely laminar nor completely turbulent. Additionally, literature mentions plug flow, a low-velocity, sub-laminar condition where the fluid moves as a homogeneous, relatively undisturbed body. However, this flow regime is rarely dominant in modern well cementing, except in very large holes. Turbulent flow of cement slurry is preferred in well cementing because it enhances the efficiency of cement displacement to drilling fluids. Identifying flow regimes involves Reynolds number analysis for the specific fluid involved.

II.5 Model selection

The characterization of rheological properties of cement slurries and other oil field fluids is typically performed using a coaxial cylinder viscometer, as described by Savins and Roper in 1954. This device consists of a large cup containing the test fluid, an outer sleeve (rotor), and an inner cylinder (bob). The rotor spins at various speeds, and the bob, attached to a torsion spring, measures the torque exerted by the fluid. The deflection of the torsion spring is read on a dial, which is then converted to shear stress and shear rate.

The rotor-and-bob geometry has specific dimensions, and the outer sleeve can rotate at multiple speeds, covering a shear-rate range from 5 sec^{-1} to 1022 sec^{-1}. Six-speed models are common (600, 300, 200, 100, 6, and 3 rpm), while twelve-speed models are preferred for more detailed analysis. The test procedure involves measuring the instrument-dial readings at various speeds, converting these to shear stress and shear rate, and generating a shear-stress/shear-rate plot to determine the rheological model and fluid parameters.

The slurry is prepared following a specific procedure and preconditioned in a consistometer to reach the desired temperature and pressure. After preconditioning, the slurry is transferred to the viscometer and sheared at different speeds to record torque readings. This process, known as a hysteresis loop, helps detect time-dependent effects like thixotropy.

At any given rotational speed, Ω, the ramp-up/ramp- down dial readings, θ, are averaged and then converted to shear rates and shear stresses at the inner cylinder (bob) using the following equations:

$$\gamma = 1.705 \times \Omega \qquad .(2.19)$$

$$\tau = 1.067 \times \theta \qquad .(2.20)$$

Rotational speed	Ramp-up dial readings	Ramp-down dial readings	Average readings	Shear rates	Shear stresses
300	97	97	97	511.5	103.5
200	69	70	69.5	341	74.16
100	39	39	39	170.5	41.61
60	27	26	26.5	102.3	28.28
30	18	16	17	51.15	18.14
6	9	7	8	10.23	8.54
3	8	5	6.5	5.12	6.94

Table II.1: Viscometer Readings for a Cement Slurry

The data were then plotted and analyzed (**Figure II.10**).

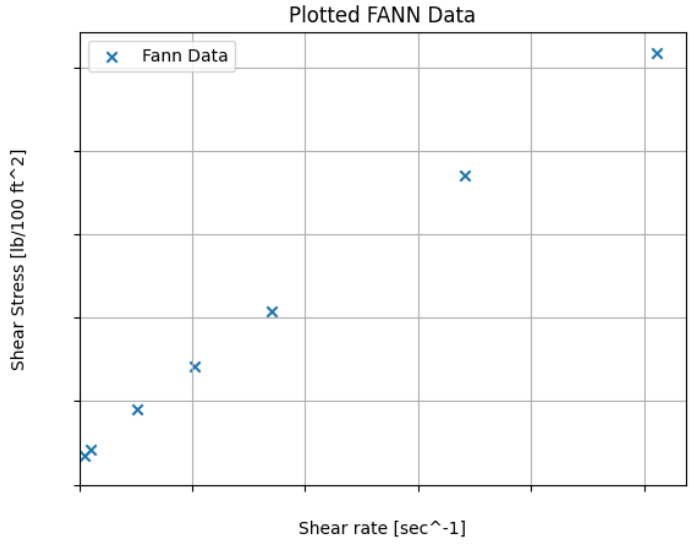

Figure II.10: Plotted data points

After plotting the data, we use linear algebra to curve fit each rheological model corresponding to the respective model equations (**Equations 2.3, 2.7, and 2.11**). This allows us to obtain the

parameters for each model and calculate the correlation coefficient r from **Equation 2.21** for each graph (See **Figure II.11**).

$$r = \frac{n(\sum_{i=0}^{n} x_i y_i) - (\sum_{i=0}^{n} x_i)(\sum_{i=0}^{n} y_i)}{\sqrt{[n(\sum_{i=0}^{n} x_i^2) - (\sum_{i=0}^{n} x_i)^2)] \times [n(\sum_{i=0}^{n} y_i^2) - (\sum_{i=0}^{n} y_i)^2)]}} \quad .(2.21)$$

where

- $\boldsymbol{n}$ is the number of pairs of scores,
- $\sum_{i=0}^{n} \boldsymbol{x_i y_i}$ is the sum of the products of paired scores,
- $\sum_{i=0}^{n} \boldsymbol{x_i}$ and $\sum_{i=0}^{n} \boldsymbol{y_i}$ are the sum of the scores and scores respectively,
- $\sum_{i=0}^{n} \boldsymbol{x_i^2}$ and $\sum_{i=0}^{n} \boldsymbol{y_i^2}$ are the sum of the squared scores and scores respectively.

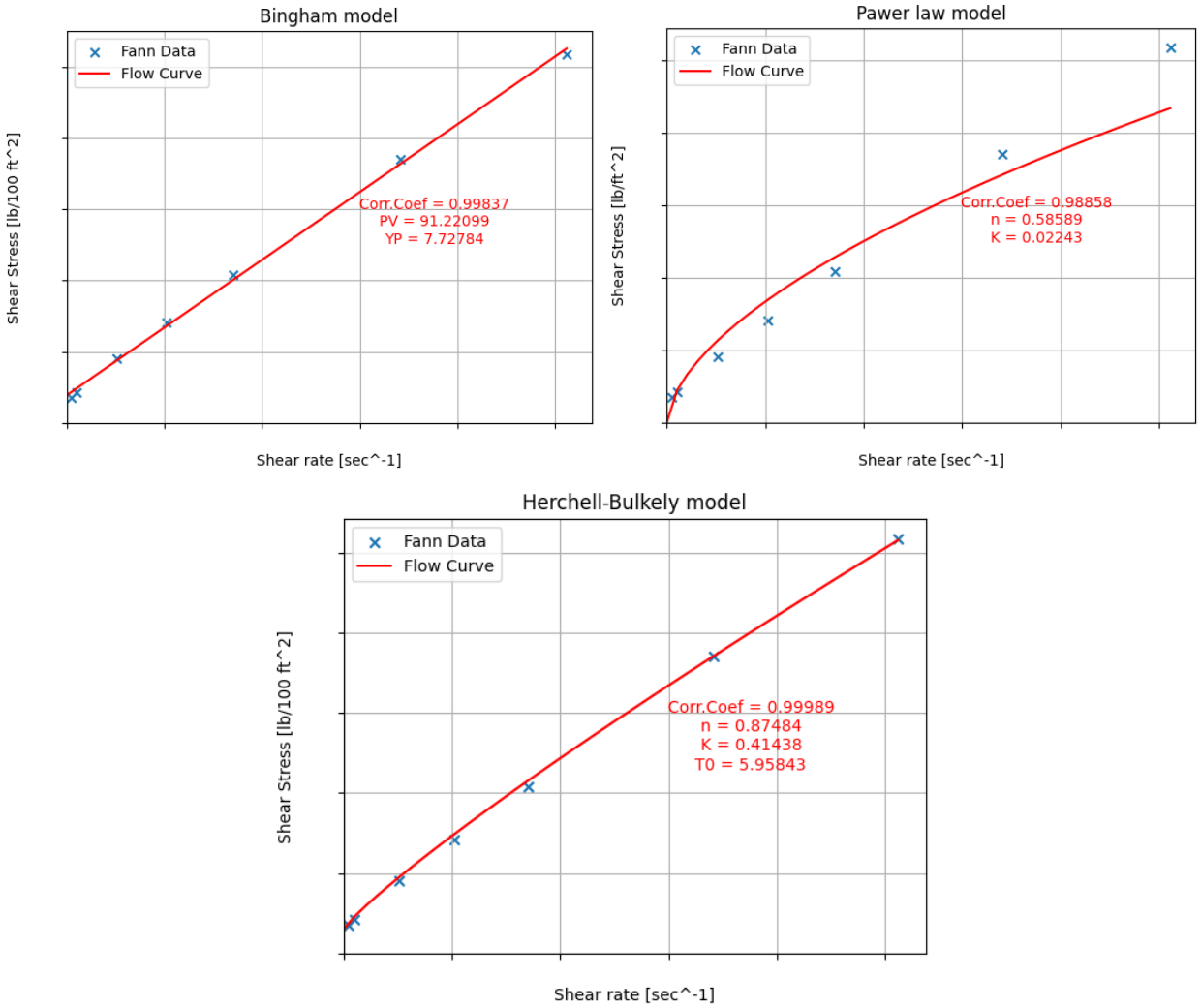

Figure II.11: Different flow curve for different rheological models

Despite its imperfections, the Bingham plastic model more accurately represents the rheological behavior of the cement slurry more than pawer law model which can be . This example underscores the common limitations of such models in capturing the rheology of cement slurries. The Bingham plastic model often overestimates shear stresses at low shear rates, whereas the power-law model can result in significant inaccuracies throughout the shear-rate range. Specifically, the power-law model typically underestimates shear stresses at both low and high shear rates, while overestimating them at intermediate values. It seems that the Herschel-Bulkley model is the best in terms of fitting the data because it has the highest correlation coefficient.

CHAPTER III

SOFTWARE CORE FUNCTION & DESCRIPTION

III.1. Cement Job Simulations

Computer-assisted design for primary cementing is crucial for cementing engineers to ensure successful cementing and zonal isolation. This design employs a computer program to analyze various aspects of the cement job. Several computer cementing simulators are available, including Schlumberger's CEMENTICS, Baker Hughes' CemFACTS, and Halliburton's iCEM. These simulators often feature branded and standalone modules within their software packages, with detailed information about their submodules and capabilities available on the providers' websites.

In addition to these, there are numerous other numerical simulators that assist cementing engineers in designing a cement job. Given the short duration of cement jobs, these simulations are typically transient rather than steady-state. They generally fall into categories such as hydraulic (including U-tubing) and temperature simulators, with other useful simulations covering stress, drilling, casing and drill string, and acoustic properties. Cement simulation is often thought of as only hydraulics simulation, however detailed data input is required for accurate hydraulic simulation. The objectives of the cement job will determine which additional steps are necessary beyond the hydraulic simulation. Often, the design and simulation of a cement job require an iterative process that may involve designing additional fluids or redesigning the pump schedule to meet all cement job objectives.

Cement job simulation is a workflow process that integrates into the well design process, can be revisited during drilling, and repeated post-job for evaluation. This adaptable workflow suits most cementing simulation exercises. Simulation results can be visualized or plotted against time or depth in the wellbore. The detail of these simulations and visualizations depends on computer capabilities. This chapter introduces how calculations are performed in our software, which can plot basic parameters like pressures and densities (hydraulic density and equivalent circulating density) and annular displacement in the wellbore. Typical simulator outputs can include also spacing/standoff and centralization plots, which help evaluate whether the cement job objectives are achieved.

III.2. Modeling

To model the behavior of the pressure and flow dynamics in a well, a suitable hydraulic model is necessary. The derivation of such a hydraulic model is based on one main assumption, the fluid in the well can be treated as a viscous fluid. The derivations in this section is mainly based on Merritt (1967)[14] and White (2011) [15]. By assuming a viscous fluid. whether it is spacer, fluid or cement flowing in the well, the flow behavior can be fully described by the following fundamental equations:

- **Fluid viscosity:** The fluid viscosity is a function of temperature and pressure but this dependence on temperature and pressure is negligible.
- **Equation of states:** The fluid density, is a function of temperature and pressure.
- **Equation of continuity:** Conservation of mass.
- **Conversation of momentum:** Newton's second law of motion or the force balance .

- **Equation of energy:** The first law of thermodynamics or the energy balance, but the development of a simplified model for the transient temperature effects will not be discussed here.

One of the biggest challenges in modeling is to make the model as simple as possible without neglecting important factors. The hydraulic model presented in this section is a simplified hydraulic model, capable of estimating pressure and flow dynamics during a cement operation. The model is based on the work of Stamnes et al. (2012) [16] and Kaasa et al. (2012) [17].

However, some modifications are done in order to make it suitable for the control system likewise Stamnes et al. (2012) [16] focused on pressure dynamics in the drill string, incorporating compressibility into their mass balance equations. However, unlike their model, our model diverges by considering compressibility effects of drilling mud in the annulus also, given its pressurized nature owing to its isolation from the atmosphere., The flow rate from the drill string to the annulus modeled based on a momentum balance. The mass balance leads to a volume balance, alongside the pressure distribution throughout the well/drill string.

During the outlining of this hydraulic model, several assumptions were made:

- **Isothermal Condition:** Temperature remains constant throughout the operation, allowing the neglect of the equation of energy.
- **Radially Homogeneous Flow:** Properties are averaged over the cross-section of the flow.
- **One-Dimensional Flow:** Only one-dimensional flow along the well is considered.
- **Constant Viscosity:** Variance in viscosity over time is disregarded.
- **Incompressible Flow:** Spatial and temporal variance of density is neglected in the momentum equation. However, key compressibility effects of the fluid are accounted for by integrating the equation of state with mass conservation.

III.2.1. Equation of state

The equation of state may in general be written as

$$\rho = \rho(P,T) \qquad .(3.1)$$

In contrast to the ideal gas law which is derived from the kinetic theory of gases, the equation of state cannot be mathematically derived from physical principles. In general, measured PVT data may be used to obtain an empirical map of pressure and temperature dependency which can be interpolated (See e.g. Isambourg et al. (1996) [18]). Since the changes in density as a function of pressure and temperature are small for a liquid, it is common to use the linearized equation of state

$$\rho = \rho_0 + \frac{\rho_0}{\beta}(P - P_0) - \rho_0\alpha(T - T_0) \qquad .(3.2)$$

where

$$\beta = \rho_0 \left(\frac{\partial P}{\partial \rho}\right)_T \qquad .(3.2A)$$

$$\alpha = -\frac{1}{\rho_0}\left(\frac{\partial \rho}{\partial T}\right)_P \qquad .(3.2B)$$

Here, ρ_0, P_0, and T_0 define the reference point for the linearization, while β is called the isotermal bulk modulus of the liquid, and α is the cubical expansion coefficient of the liquid. In general, the accuracy of the linearized equation of state reduces with increasing pressure and temperature ranges, but can be said to be accurate for most drilling fluids for pressure ranges 0–500 bar, and temperature ranges 0–200 °C. This can be verified by experimental PVT data (e.g. in Isambourg et al. (1996) [18]).

In the following, Kaasa et al. (2012) [17] derive a simplified dynamic model for the pressure transients in the system based on the following differential form of (3.2)

$$d\rho = \frac{\rho_0}{\beta} dp \qquad .(3.3)$$

Where they neglect dependence on the temperature. Even though significant temperature gradients may exist, the thermal expansion coefficient α for liquids is usually small, thus density changes due to temperature changes are in many cases negligible with respect to transient effects. Furthermore, since transient temperature effects are relatively slow compared to the pressure transients of the system, such effects are usually more effectively handled by online calibration based on feedback from measurements.

III.2.2. Equation of continuity

For one-dimensional flow, the differential continuity equation can be expressed as

$$\frac{\partial \rho}{\partial t} + \frac{\partial}{\partial x}(\rho v) = 0 \qquad .(3.4)$$

where v is the velocity of the flow, and x is the spatial variable along the flow path. Assuming the cross-section of the flow $A(x)$ is piecewise constant, Equation (3.4) is similar to the one used in advanced hydraulic models. Note also that by using Equation (3.3), we can rewrite Equation (3.4) as

$$\frac{\partial P}{\partial t} = -\frac{\beta \partial q}{A \partial x} \qquad .(3.5)$$

with pressure P and volumetric flow rate q as variables, which is a form commonly used to describe incompressible pipe flow (Goodson and Leonard 1972[19], Stecki and Davis 1986[20]).

The assumption of incompressible flow only means we have neglected the effect of density in the characteristics of the flow. The main compressibility effects of the fluid are taken into account due to the equation of state and the continuity equation. This property characterizes the dominating dynamics of the hydraulic system, and is reflected in the pressure along the entire

flow path. The dynamics of a pressure at any point in the well can thus be approximated quite accurately by the dynamics of the average pressure in the entire well, offset with the hydrostatic pressure and friction drop relative to some fixed reference point. A dynamic model for the pressure based on this approximation is derived in the following paragraph.

From (3.4) we can integrate over a control volume V and get the mass balance in integral form

$$\frac{d}{dt}(\rho V) = \rho_{in} q_{in} - \rho_{out} q_{out} \qquad .(3.6)$$

where ρ is the average density, and $w_{in} = \rho_{in} q_{in}$ and $w_{out} = \rho_{out} q_{out}$ are the flow rate of mass in and out of the control volume V, respectively. To obtain a more convenient form, we can rewrite (3.6) using (3.3) to get pressure as the main variable according to

$$\rho \frac{V}{\beta} \frac{dP}{dt} = -\rho \frac{dV}{dt} + \rho_{in} q_{in} - \rho_{out} q_{out} \qquad .(3.7)$$

where P is the average pressure in the control volume, and q_{in} and q_{out} are the volumetric flow rates, with inlet density ρ_{in} and ρ_{out}, respectively. Equation (3.7) can be used to approximate the dominating dynamics of the hydraulic system.

III.2.3. Equation of momentum

The main effect of flow will be treated as one-dimensional assumption is that the differential equation momentum for incompressible flow reduces from three to one dimension, which is much simpler, but still relatively accurate with respect to averaged flow variables White (2011)[15]. The resulting partial differential equation can be written as

$$\rho \frac{dv}{dt} = -\frac{\partial P}{\partial x} + \frac{\partial \tau}{\partial x} - \rho g \cos \emptyset \qquad .(3.8)$$

where x is the spatial coordinate along the flow path, v the velocity of the flow, τ is the viscous force per unit, and $\emptyset$ is the angle of the flow path. Equation (3.8) is similar to the one used in advanced hydraulic models (See e.g. Petersen (2008)[21]). Using the fact that $A(x)$ is piecewise constant, we can rewrite (13) with flow rate q as main variable according to

$$\frac{\rho}{A} \frac{dq}{dt} = -\frac{\partial P}{\partial x} + \frac{\partial \tau}{\partial x} - \rho g \cos \emptyset \qquad .(3.9)$$

Assuming the fluid accelerates homogeneously as a stiff mass, Equation (3.9) can be integrated along the flow path to obtain a simple equation for the average flow rate dynamics according to

$$M(l_1, l_2) \frac{dq}{dt} = P_1 - P_2 - F(l_1, l_2, q, \mu) - G(l_1, l_2, \rho) \qquad .(3.10)$$

where

$$M(l_1, l_2) = \int_{l1}^{l2} \frac{\rho(x)}{A(x)} dx \qquad .(3.10A)$$

$$G(l_1, l_2) = \int_{l1}^{l2} \rho(x) g \cos \emptyset(x)\, dx \qquad .(3.10B)$$

Here, q is the average flow rate of the fluid in the control volume between the spatial coordinate $x = l1$ to $x = l2$ of the flow path, P_1 is the pressure at $x = l1$, and P_2 is the pressure at $x = l2$. Furthermore, the parameter $M(l_1, l_2)$ is the integrated density per cross-section over the flow path, $F(l_1, l_2, q, \mu)$ is the friction along the flow path, and $G(l_1, l_2)$ is the total gravity affecting the fluid. Equations (3.10) & (3.10B) can be used to approximate the flow dynamics of the hydraulic system.

III.3. The Simplified Hydraulic Model

A simple hydraulic model of a well can be obtained using (3.7) and (3.10) through (3.10B), derived in the previous section, combined with an accurate steady-state characteristics of the downhole pressure, P_{dh}. To further simplify the presentation here, we assume

$$\rho = \rho_{in} = \rho_{out} \qquad .(3.11)$$

First, consider the flow in the drill string from mud pump to the bit as our first control volume, and let the mud pump pressure P_p be described by (3.7) according to

$$\frac{V_p}{\beta_p}\frac{dP_p}{dt} = q_p - q_s \qquad .(3.12)$$

where V_p is the volume of the drill string, β_p is the effective bulk modulus, q_p and q_s are the pump flow and flow through the shoe, respectively. Notice that the densities have cancelled out due to Equation (3.11), and that the volume of the drill string and annulus is constant during cementing, such that time-derivative $^{dV}/_{dt}$ is zero. Similarly, we consider the flow in the annulus from the shoes and up the well. Let the upstream down hole pressure be described by (3.7) according to

$$\frac{V_a}{\beta_a}\frac{dP_{dh}}{dt} = q_s - q_{out} \qquad .(3.13)$$

The hydrostatic pressure difference between the casing and the annulus must overcome the choke pressure and the friction in the entire well before free-fall is initiated. This scenario can be expressed as:

$$G_p(l_{fp}, l_{bit}) - F_p(l_{fp}, q) - F_a(l_{bit}, l_{fa}, h_r, q) - G_a(l_{bit}, l_{fa}, h_r) \neq 0 \qquad .(3.14A)$$

$G_p(l_{fp}, l_{bit})$,$F_p(l_{fp},q)$ represent the hydrostatic pressure and the frictional pressure loss in the drill string, respectively. Similarly, for the annulus, we have $F_a(l_{bit}, l_{fa},h_r,q)$,$G_a(l_{bit}, l_{fa},h_r)$

$$hd = \frac{q_s - q_p}{A_p}$$

To implement (3.12) and (3.13) it is necessary to provide a relationship for calculating the volume of the different fluids. To that end we assume that the drill string or annulus is filled with two different fluid with two different initial control volumes in each case, V_{p1} , V_{p2}, V_{a1} , V_{a2}. Neglecting compressibility effects the volumes are given as the solution to:

$$V_{p1}{}^c = q_p \quad .(3.15A), \qquad V_{p2}{}^c = -q_s \quad .(3.15B)$$

$$V_{a1}{}^c = -q_{out} \quad .(3.15C), \qquad V_{a2}{}^c = q_s \quad .(3.15D)$$

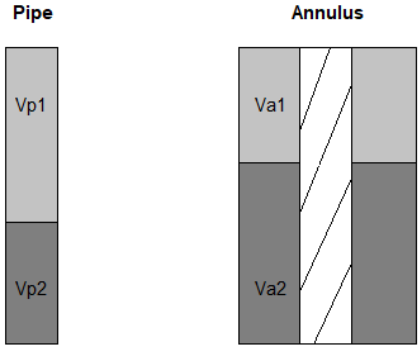

Figure III.1: Fluid volumes in pipe / annulus

However, due to compressibility effects the above equations (3.15A/B) and (3.15C/D) are not valid during transients so to take the different compressibilities into account for more accurately normalize the volume calculations we use the bulk modulus, which for Fluid 1 is defined as

$$\beta_{p1} = -V_{p1}{}^c \frac{\Delta p}{V_{p1} - V_{p1}{}^c} \quad .(3.16)$$

That is, for a given pressure difference Δp the volume is compressed from $V_{p1}{}^c$ to V_{p1}, where $V_{p1}{}^c$ is the solution to (3.15A). Rearranging we get

$$V_{p1} = -V_{p1}{}^c\left(1 - \frac{\Delta p}{\beta_{p1}}\right) \quad .(3.17A)$$

Similarly for fluid 2 we have

$$V_{p2} = -V_{p2}{}^c\left(1 - \frac{\Delta p}{\beta_{p2}}\right) \quad .(3.17B)$$

where $V_{p2}{}^{c}$ is the solution to (3.15B). In the above equations we have three unknowns V_{p1}, V_{p2} and Δp and it is therefore necessary to add an additional relationship. For this purpose we use the knowledge that the known drill string volume V_p, satisfies $V_p = V_{p1} + V_{p2}$

We now have three independent equations so we can solve for the three unknowns. So after we calculate the compressible volumes of our fluids we can Δp can calculated by:

$$\Delta p = \frac{V_p - (V_{p1}{}^{c} + V_{p2}{}^{c})}{\frac{V_{p1}{}^{c}}{\beta_{p1}} + \frac{V_{p2}{}^{c}}{\beta_{p2}}} \qquad .(3.18)$$

After that we can use (3.17A) & (3.17B) to provide volumes for the implementation of (3.12) and we follow the same steps for the implementation of (3.13). To model the flow rate through the bit Stamnes[18] 2012 use a momentum balance similar to the one in equation (3.10) giving:

$$M(h_r)\frac{dq_b}{dt} = P_p - P_0 - F(l_{fp}, l_{fa}, h_r, q) + G(l_{fp}, l_{fa}, h_r) \qquad .(3.18)$$

Where:

$$M(h_r) = \int_0^{l_{bit}} \frac{\rho_p(x)}{A_p(x)}\,dx + \int_{h_r}^{l_{bit}} \frac{\rho_a(x)}{A_a(x)}\,dx \qquad .(3.18A)$$

$$F(l_{fp}, l_{fa}, h_r, q) = F_p(l_{fp}, q) + F_a(l_{bit}, l_{fa}, h_r, q) \qquad .(3.18B)$$

$$G(l_{fp}, l_{fa}, h_r) = G_p(l_{fp}, l_{bit}) - G_a(l_{bit}, l_{fa}, h_r) \qquad .(3.18C)$$

where P_0 is the gauge Pressure, $F(l_{fp}, l_{fa}, h_r, \mu)$ is the total frictional pressure loss in the drill string and annulus, $G(l_{fp}, l_{fa}, h_r)$ describes the hydrostatic pressure difference between the drill string and the annulus, $\rho_p(x)$ and $\rho_a(x)$ are the densities, at location x, in the drill string and annulus respectively, l_{bit} is the length from the rig floor to the bit and finally $A_p(x)$ and $A_a(x)$ are the cross sectional areas, at location x, in the drill string and annulus respectively. Note that F and G depend on additional parameters such as geometry and density. These arguments are omitted for notational convenience. More detailed expressions for these functions are given in (3.18B) and (3.18C). So the flow in casing shoe and the flow from the well can giving as:

$$M(h_r)\frac{dq_s}{dt} = P_p - P_0 - F(l_{fp}, l_{fa}, h_r, q) + G(l_{fp}, l_{fa}, h_r) \qquad .(3.19)$$

$$M_a(l_{bit}, h_r)\frac{dq_{out}}{dt} = P_{dh} - P_0 - [F_a(l_{bit}, l_{fa}, h_r, q) + G_a(l_{bit}, l_{fa}, h_r)] \qquad .(3.20)$$

Frictional Pressure Loss P_{loss}

Cementing fluids are generally non-Newtonian, and the flow path involves both laminar and turbulent flow regimes, with transitions between these regimes. This complexity makes detailed modeling of frictional losses a significant challenge. For high accuracy, the Herschel-Bulkley model is the industry standard specially cement slurries. The modeling framework presented thus far allows for any functional description of the pressure losses, including non-Newtonian models.

However, for the sake of challenge, we will restrict ourselves to the non-Newtonian models mentioned earlier. For completeness, we state the main relationships and explain how we use them.

The most important technical parameters in simulation is the pressure drop as it influences the requirement of pumping energy. The pressure drop is produced by the internal friction of the slurry and friction between the pipe and the slurry. This interaction is commonly expressed as a dimensionless factor called friction factor. This friction factor is found to be a function the Reynolds number which in turn primarily depends on the slurry properties (velocity, density, and viscosity). We use empirical relationships that considered to be used in all flow regimes.

- **Bingham plastic model**

At times, it is necessary to have a data correlation that covers the entire range of Reynolds numbers from laminar flow through transitional flow to the highest Reynolds numbers. To address this, Morrison (2013)[22] developed a new data correlation for smooth pipes that is explicit and relatively simple in form. According to Assefa et al. (2015) [23], this is the only equation representing the friction factor for all flow regimes within a single equation. The authors recommend using this correlation for estimating the friction factor of Bingham fluids. Consequently, we rely on this correlation to calculate the friction factor for our fluids.

$$C_f = \frac{16}{R_{eBP}} + \left[\frac{0.0076\left(\frac{3170}{R_{eBP}}\right)^{0.165}}{1+\left(\frac{3170}{R_{eBP}}\right)^{7}}\right] \qquad .(3.21)$$

Where:

For pipe: $R_{eBP} = 928 \times \frac{\rho v d}{\mu_a}$.(3.21A) **and** $\mu_a = \mu_p \times \frac{6.66\tau_y d}{v}$.(3.21C)

For annulus: $R_{eBP} = 757 \times \frac{\rho v(d_h - d_p)}{\mu_a}$.(3.21B) **and** $\mu_a = \mu_p \times \frac{5\tau_y(d_h - d_p)}{v}$.(3.21D)

- **Power law model**

To calculate friction pressure losses, the friction factor must be determined first, partly due to the many correlations available for predicting the friction factor in non-Newtonian pseudoplastic shear-thinning fluids. These models are generally developed for specific types of materials or based on particular sets of results, making them not universally applicable[24]. There are no general theories or comprehensive mathematical and computational models to describe turbulent flow[25]. Instead, various analytical, semi-empirical, and empirical correlations (both explicit and implicit) have been proposed to predict the friction factor under turbulent flow conditions[24]. According to AH Kamel et al. (2018) [26], the equation by El-Emam et al. (2003) [27] is more accurate than all other equations used in their study when considering some specific criterions.

$$f = \frac{n}{3.072-0.143n} R_{ePL}^{\frac{n}{0.282-4.211n}} - 0.00065 \qquad .(3.22)$$

Where:

- **For pipe:** $R_{ePL} = 89100 \times \frac{\rho v^{2-n}}{K} \times \left(\frac{0.0416d}{3+\frac{1}{n}}\right)^{n}$.(3.22A)
- **For annulus:** $R_{ePL} = 109000 \times \frac{\rho v^{2-n}}{K} \times \left(\frac{0.0208(d_h - d_p)}{2+\frac{1}{n}}\right)^{n}$.(3.22B)

- **Herschel-Bulkley model**

In our calculation, we use the friction factor based on the Unified model by Zamora et al. (2005)[28]. As mentioned earlier, this model is an enhanced version of the simplified Herschel-Bulkley model. The primary objective of their work is to prevent advanced hydraulic software applications from becoming "black boxes" for field engineers and this was a challenge we needed to overcome. The relationships are already in use by at least part of the drilling industry, and are all direct and simple enough to use in a spreadsheet without complicated macros.

We start with Herschel-Bulkley model parameters n, K from these oilfield rheological measurements using the equations (2.15) and (2.16) for pipe flow and equations (2.17) and (2.18) for annulus flow and τ_y is derived from the equation (2.12). Then we calculate the mean velocity v for both the pipe and annulus, considering the respective flow rate q.

$$v = \frac{24.54 \times q}{d^2} \quad .(3.23A)$$

$$v = \frac{24.54 \times q}{d_h{}^2 - d_p{}^2} \quad .(3.23B)$$

The shear rate at the wall γ_w, is determined by multiplying the Newtonian shear rate by a geometry factor G. This calculation is applicable to pipes and annulus given the appropriate values for fluid velocity v and hydraulic diameter d_{hyd}.

$$\gamma_w = \frac{1.6Gv}{d_{hyd}} \quad .(3.24) \text{ where } \quad G = \left[\frac{(3-\alpha)n+1}{(4-\alpha)n}\right]\left[1 + \frac{\alpha}{2}\right] \quad .(3.24A)$$

Factor G is dependent on the rheological parameter n and a geometry factor $\alpha = 0$ for pipes and $\alpha = 1$ for annulus. Frictional pressure loss is an increasing function of the shear stress at the wall τ_w defined by the fluid-model-dependent flow equation. Flow equations for Herschel-Bulkley fluids are complex and can be approximated by the Unified model flow equation that is of the same recognizable form as the respective constitutive equations.

$$\tau_w = 1.066\left[\left(\frac{4-\alpha}{3-\alpha}\right)^{n}\tau_y + K\gamma_w{}^{n}\right] \quad .(3.25)$$

Then involving the shear stress at the wall τ_w the most convenient form to calculate a generalized Reynolds number R_{eG} is used to define the flow regime and to determine the friction factor of the equation.

$$R_{eG} = \frac{\rho V^2}{19.36\,\tau_w} \quad .(3.26)$$

Then we calculate the friction factor for each flow regime (Laminar-flow, Transitional-flow, Turbulent-flow) using the generalized Reynolds number R_{eG} defined in Eq. 8.

$$f_{lam} = \frac{16}{R_{eG}} \quad .(3.27) \qquad f_{trans} = \frac{16\,R_{eG}}{(3470-1370n)^2} \quad .(3.28)$$

$$f_{lam} = \frac{a}{{R_{eG}}^b} \quad .(3.29)$$

Where: $a = \frac{\log_{10}(n_p) + 3.93}{50}$.(3.29A) $b = \frac{1.75 - \log_{10}(n_p)}{7}$.(3.29B)

Pressure losses in pipes and annulus are proportional to the Fanning friction factor f that will be calculated as a final step to included losses equation. In turn is a function of generalized Reynolds number, flow regime, and fluid rheological properties use a technique involves an intermediate term f_{int} based on transitional and turbulent-flow friction factors f_{trans} and f_{turb}, respectively, and the laminar-flow friction factor flam

$$f = \left({f_{int}}^{12} + {f_{lam}}^{12}\right)^{\frac{1}{12}} \quad .(3.30)$$

Where:

$$f_{int} = \left({f_{trans}}^{-8} + {f_{turb}}^{-8}\right)^{\frac{-1}{8}} \quad .(3.31)$$

As long as the fluid temperature does not change appreciably in the main test section. The following equation also can be used as we do to calculate pressure losses in actual wells if allowances are made for geometrical changes and the effects of temperature and pressure on downhole rheological properties and density[29].

$$P_{loss} = \frac{1.076\,\rho\,V^2\,L\,f}{d_{hyd}\,10^5} \quad .(3.32)$$

III.4. Technologies

As a programming language, we use Python due to its versatility and power, making it widely adopted across various fields, including scientific computing, data analysis and simulation software. Python is renowned for its readability and simplicity, which allows developers to write clear and concise code. This quality makes Python an excellent choice for complex simulations and data-intensive applications. Its capabilities are particularly advantageous for developing simulation software, especially in the context of cementing simulations for oil and gas wells. Python offers several key features that enhance its suitability for this purpose:

- **Ease of Learning and Use:** Python's straightforward syntax makes it easy to learn, allowing developers to focus more on problem-solving rather than grappling with complex language constructs.
- **Extensive Libraries and Frameworks:** Python has a rich ecosystem of libraries and frameworks. We utilize many of these, such as NumPy for numerical computations, Pandas for data manipulation, Matplotlib for data visualization, and SciPy for scientific and technical computing. These libraries significantly enhance productivity by handling complex mathematical operations and creating detailed plots and visualizations of simulation results, enabling the development of robust simulations that help understand and interpret data effectively.

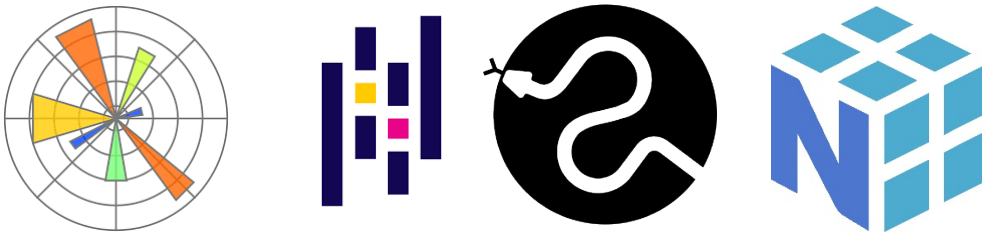

Figure III.2: Matplolib, Pandas, Scipy, Numpy Logos, respectively

- **Strong Community Support:** Python benefits from a large and active community of developers and researchers who contribute to its continuous improvement. This support network provides a wealth of resources, including documentation, tutorials, and forums, making it easier to find solutions and stay updated with the latest advancements.
- **Object-Oriented and Functional Programming:** Python supports multiple programming paradigms, including object-oriented and functional programming. This flexibility allows developers to choose the best approach for their specific needs, enhancing the modularity and reusability of the code.

In summary, Python's combination of ease of use, extensive libraries, and strong community support makes it an ideal choice for developing sophisticated simulation software in the field of cementing engineering. This versatility ensures that we can create accurate, reliable, and efficient simulations, which are crucial for the successful cementing of oil and gas wells.

III.5. Software Description

Our software encounters several challenges throughout its workflow. Initially, it struggles to classify fluids based on their rheological properties. Once classification is complete, the software enters an iterative process, calculating changes in various parameters, such as flows, volumes, lengths, pressures, pressure loss, and free fall effect, during each iteration. This process culminates in plotting the data to extract valuable insights from each plot. When compared with the output from other software, such as CemFACTS, this detailed analysis allows us to better understand fluid dynamics, thereby improving the overall efficiency and accuracy of our system.

III.5.1. Simulation phases

III.5.1.1. Classification of fluids

The matrix used in this program includes correlations for calculating the friction factor of non-Newtonian fluids flowing in circular pipes and annular spaces under various flow conditions. Three correlations (refer to **Equations 3.21, 3.22** and **3.30**) are available in the literature to determine the friction factor for each rheological model, enabling the calculation of pressure loss. These models were chosen for their high accuracy and precision, simplicity, and broad applicability. However, some correlations are not considered in this thesis due to their complexity or limited applicability. The classification is based on the correlation factor discussed in the previous chapter (see **Equation 2.20**). Therefore, after calculating the rheological parameters for each model of each fluid used in our operation, the higher the calculated correlation factor, the more closely the fluid behavior aligns with the described model (see **Figure 2.11**).

III.5.1.2. Basic calculation

As previously discussed, the program operates an infinite loop that increments a time step counter with each iteration, stopping under specific conditions: either when the top of cement inside casing decreases until reaching the casing ring or when the spacer in the annulus runs out. During each cycle, it monitors the current simulation time and adjusts the flow rates in various parts of the cementing operation (pump, shoe, out the well). The pump's flow rate is adjusted based on predefined time intervals calculated for each fluid volume. It also performs basic calculations for other flow components, such as the flow in casing shoes and the flow from the well, according to **Equations 3.19** and **3.20**.

Additionally, the program independently manages the volumes of fluids over time, adjusting flow rates based on target conditions inside the casing and annulus. It calculates pressures both in the pump and downhole using **Equations 3.12** and **3.13**, after performing necessary calculations with Equations **3.17A** and **3.17B** to determine volumes. It then performs pressure loss calculations for the fluid columns. This comprehensive approach ensures accurate simulation and control of the fluid dynamics within the system.

III.5.1.3. Plotting the graphs and gaining insights

In conclusion, plotting the results generated by the program provides a visual representation of the fluid dynamics within the cementing operation. By graphically displaying key parameters such as flow rates, fluid volumes, and pressure changes over time, we can gain valuable insights into the system's behavior. Comparing the plotted results against predictions from other commercial software allows us to validate the accuracy and reliability of the simulation model, enhancing our understanding of how different variables interact and change throughout the simulation. This process can highlight any irregularities or expected behaviors in the cementing process, allowing discrepancies to be analyzed and used to further refine the model.

Overall, the visual representation of the simulation results through plotting is an essential tool for analyzing and enhancing the cementing operation, leading to improved performance and more informed operational decisions.

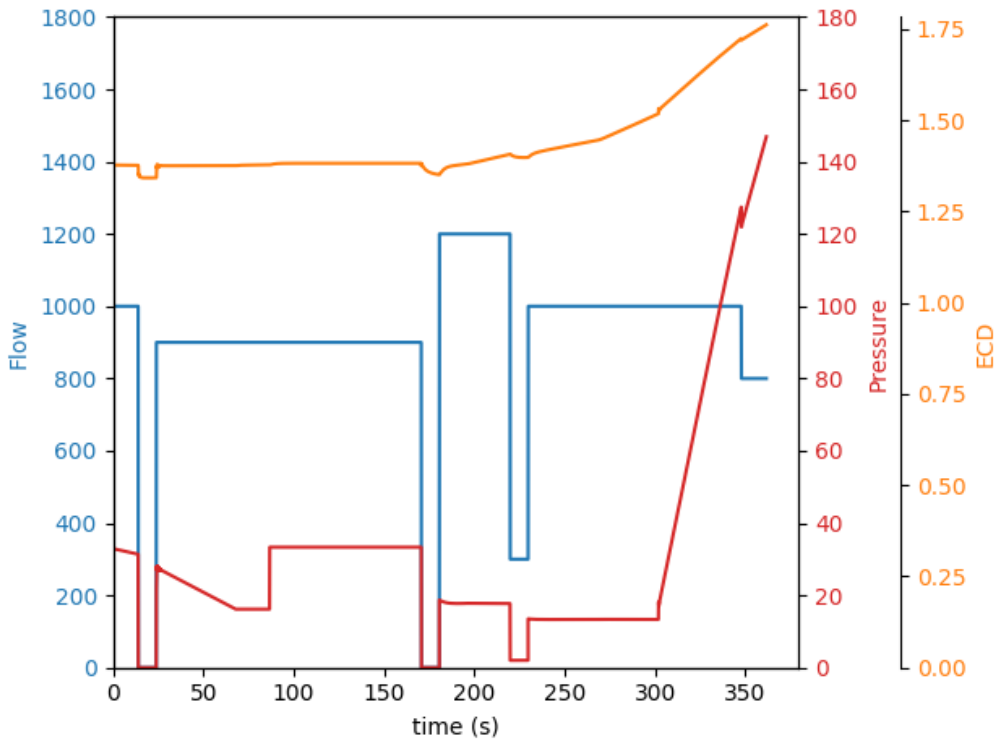

Figure III.3: A final graph generated by our program

CHAPTER IV

RESULTS & DISCUSSION

IV.1 Plotting Data

The primary objective of the simplified hydraulic model is to investigate the pressure and flow dynamics during a primary cement operation. This model, implemented in Python, simulates these dynamics to analyze the performance of the cement operation. The results from simulations for 13.375-inch casing cement operations will be compared with those obtained from the CemFACTS Simulator, using data extracted from cement reports (including fluids data, casing, and open hole data). Additionally, the limitations and drawbacks of the model simulations will be discussed. First, the data for the wells are presented, followed by a physical explanation of the behaviors observed in the simulations. The results from Python will then be compared to those from CemFACTS, and any differences will be analyzed and explained. The cement operation for 13.375-inch casing was simulated for Wells A and B, including five fluids for each well.

- **Well A**

The first well has a previous casing diameter of 17.755 inches and a previous shoe depth of 398 meters. Its TVD reaches 2306 meters with an average hole diameter of 16.4225 inches. The specific rheological fluid parameters for four different fluids are shown in the table below.

	Plastic viscosity (cP)	Yield point (lbf/hft²)	Yield Stress (lbf/hft²)	Density (kg/lt)
Spacer	26	14	/	1.4
Lead slurry	24	15	12.928	1.5
Tail slurry	84	17	8.214	1.9
Displacement	20	15	/	1.34

Table IV.1: Rheological parameters of Well A fluids

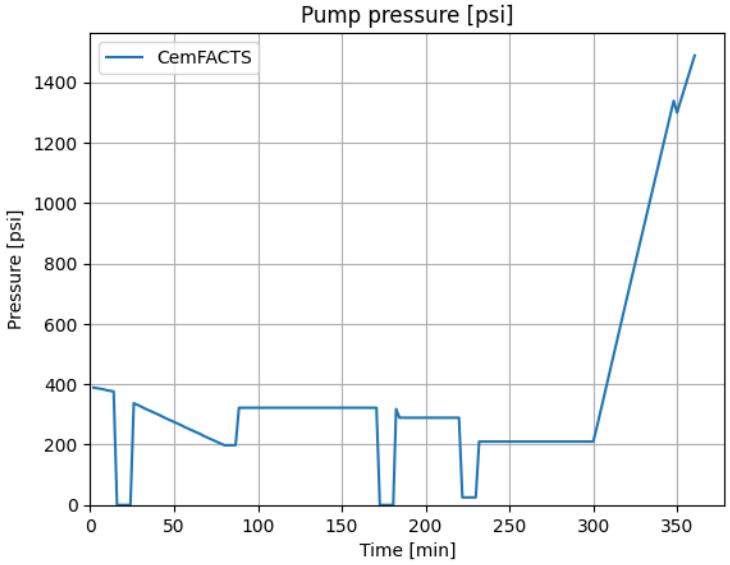

Figure IV.1: Pump pressure

At the start of the cement job simulation and like any conventional cement operation, the well is entirely filled with mud, which is considered the initial condition at **t = 0** minutes. After start pumping the increase in hydrostatic pressure leads to a corresponding decrease in pump pressure as shown in **Figure IV.1**. As heavy-weight fluid is pumped into the casing, the pump pressures continue decrease. At **t = 86.73** minutes, the pump pressure increases due to the higher surface line pressure from pumping tail slurry, which is heavier than lead slurry. The free-fall period begins when the pump pressure drops to surface line pressure, as seen in **Figure IV.4.**

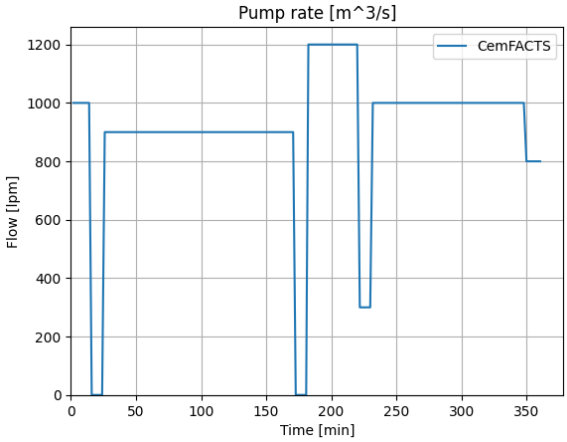

Figure IV.2: Pump rate

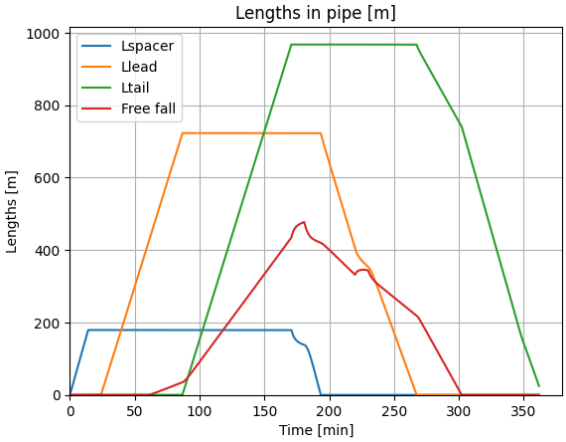

Figure IV.3: Lenths of fluids in pipe

After the planned tail volume is pumped into the casing we turn pumps off pumps, Then the displacement mud is pumped, reducing the u-tube rate due to its lower density. At **t = 225.80** minutes, the pump flow rate is reduced to 300 lpm, leading to a second increase in the air gap. The piece of software code allows for the tracking of the lengths and volumes of fluids in both the casing and annulus. Additionally, it monitors the fronts of these fluids in the casing over elapsed time. The open hole diameter was treated as two sections, the section of open hole and the section of previous casing to for the entire section (See **Figure IV.3**). The lengths and volumes of these fluids at the end of the simulation are summarized in **Table IV.2**.

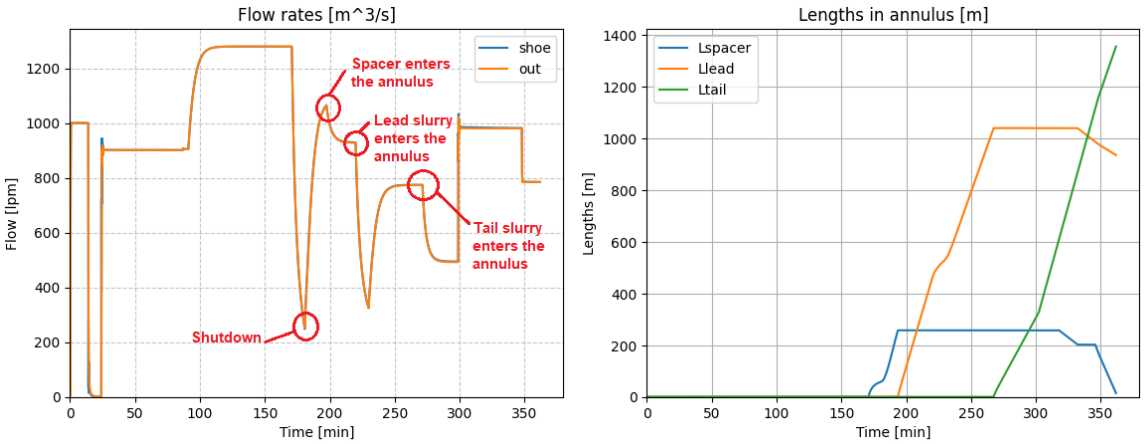

Figure IV.4: Matching between Shoe flow rate and lengths in annulus

A few minutes later, as the spacer front enters the annulus, the shoe flow and outflow rapidly decrease, as seen in **Figure IV.3**, due to the decreasing hydrostatic difference between the casing and annulus. A similar drop occurs when the lead enters the annulus at **t = 193.42** minutes. The continuous filling of the air gap increases the hydrostatic pressure, pushing the lead cement further into the annulus. Until **t = 267.26** minutes, the front of the tail cement enters the annulus, causing another rapid decrease in shoe flow and outflow. The continuous filling of the air gap raises the hydrostatic pressure. After **t = 302** minutes, the entire air gap is filled, causing a sudden increase in pump pressure. Consequently, the shoe flow and outflow increase rapidly and later stabilize slightly below the pump rate due to compressibility effects.

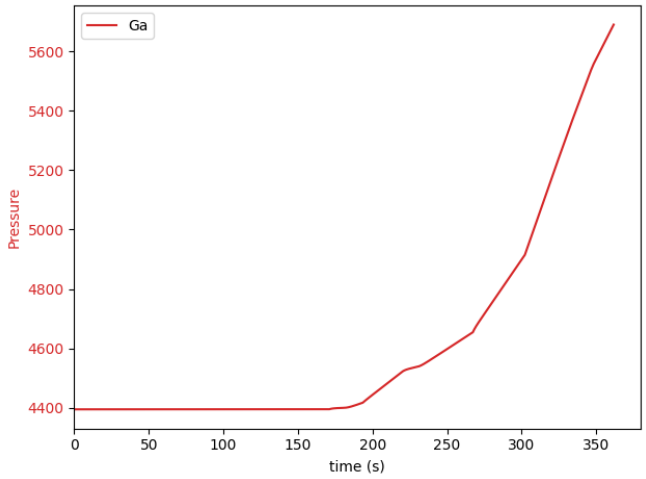

Figure IV.5: Hydrodtatic pressure

The bottom hole pressure (BHP) during the entire conventional cementing operation is plotted along with the length of the fluid columns in the annulus in **Figure IV.5**. The changes in BHP after pumping the spacer, cement, and tail are caused by flow rate changes induced by the rig pump and the u-tubing. These changes correlate directly with the behavior of the shoe and outflow rates, as seen in **Figure IV.4** and the annular friction plots as seen in **Figure IV.5**.

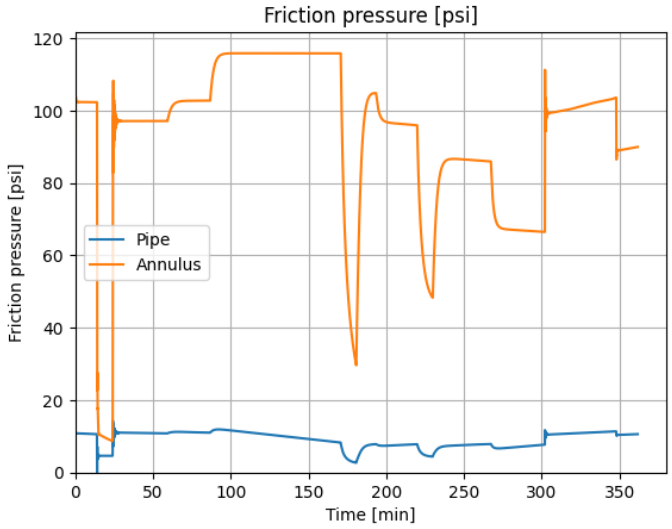

Figure IV.6: Friction Pressures

As the spacer, cement, and tail enter the annulus, the BHP increases considerably, indicating that the system is dominated by hydrostatic pressure rather than frictional pressure.

After 360 minutes, the operation is finished, and the rig pump is shut off, causing a sudden drop in BHP due to the loss of frictional pressure leaving some volume of spacer. During a conventional cement operation, the choice of cement pump rate and displacement rate can be constrained by the given pressure window. An increase in pump rate will lead to an increase in friction, raising the BHP in the annulus, as shown in **Figure IV.5**. However, these results should be compared to a reliable reference, such as the CemFACTS simulator, to measure the percentage error between the two simulation results. The next section will present this comparison procedure.

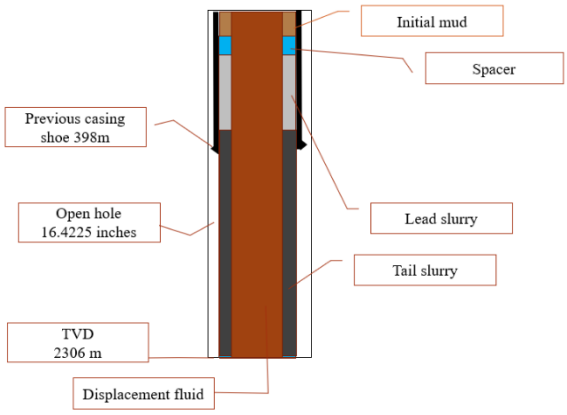

Figure IV.7: Schematic Well A description

IV.2 Comparison between results

- **Well A**

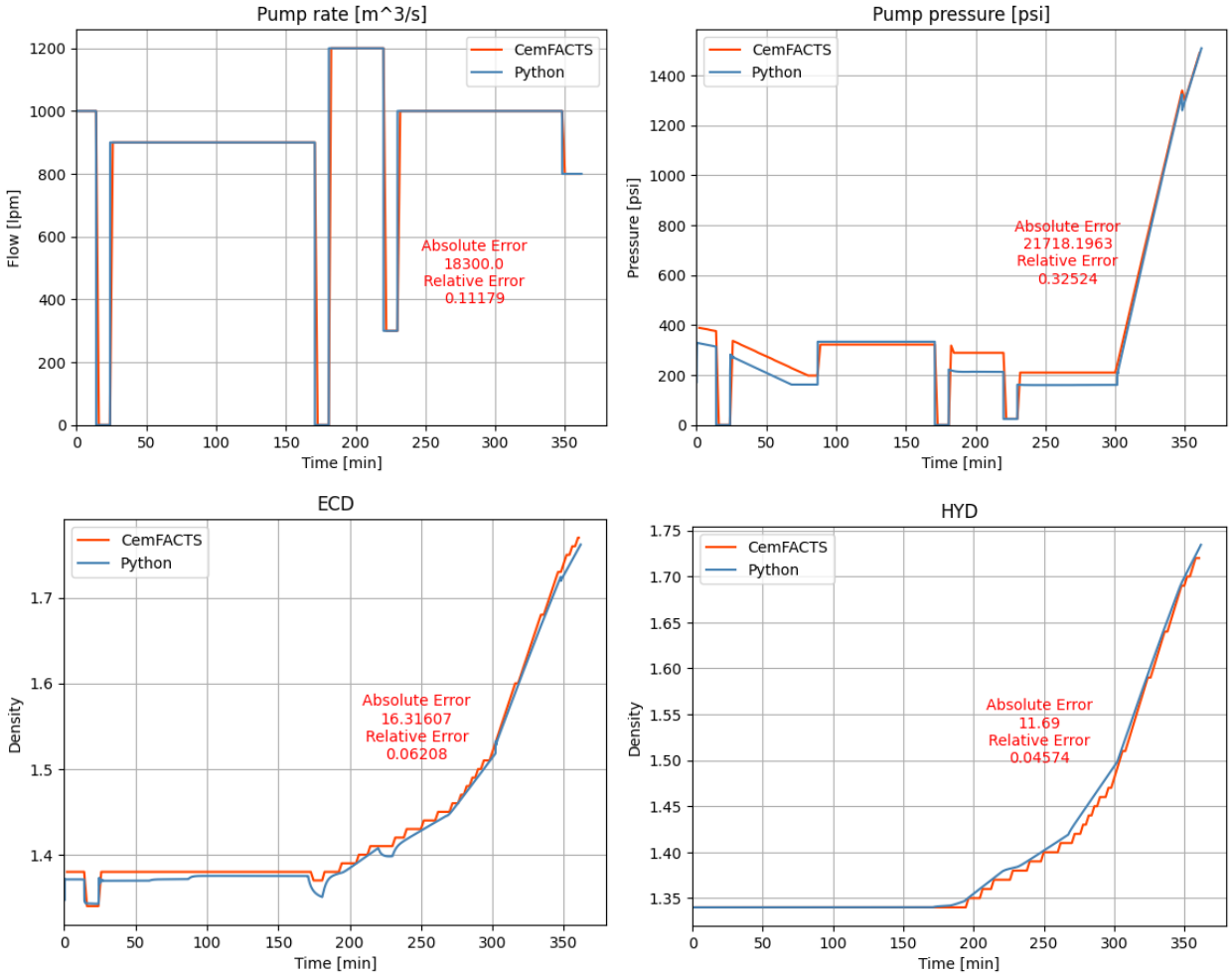

Figure IV.8: A different graphs of deferent simulation outputs (Well A)

The flow curves seems to be identical with a higher accuracy of the densities curves (a small relative error achieved) but for the pump pressure we see a major differences between the two graphs for whole time domain which we think it is because the underestimation of the friction calculation of the flow line (F_{surf}). The results of annular displacement shows in **Table 4.2.**

	Lengths (m)		Volumes (m3)	
	CemFACTS	**Python**	**CemFACTS**	**Python**
Spacer	0	0	0	0
Lead slurry	921	935.52	56.46	56.45
Tail slurry	1361	1355.68	75.56	73.58

Table IV.2: Annular displacement (**Well A**)

- **Well B**

The first well has a previous casing diameter of 17.755 inches and an average hole diameter of 16.4225 inches, with a previous shoes depth of 548 and a TVD of 2388 with specific rheological fluid parameters represented also in the table below for four different fluids.

	Plastic viscosity (cP)	Yield point (lbf/hft²)	Yield Stress (lbf/hft²)	Density (kg/lt)
Spacer	26	16	/	1.3
Lead slurry	64	10.5	12.928	1.35
Tail slurry	78	16	8.214	1.9
Displacement	19	15	/	1.25

Table IV.3: Rheological parameters of Well B fluids

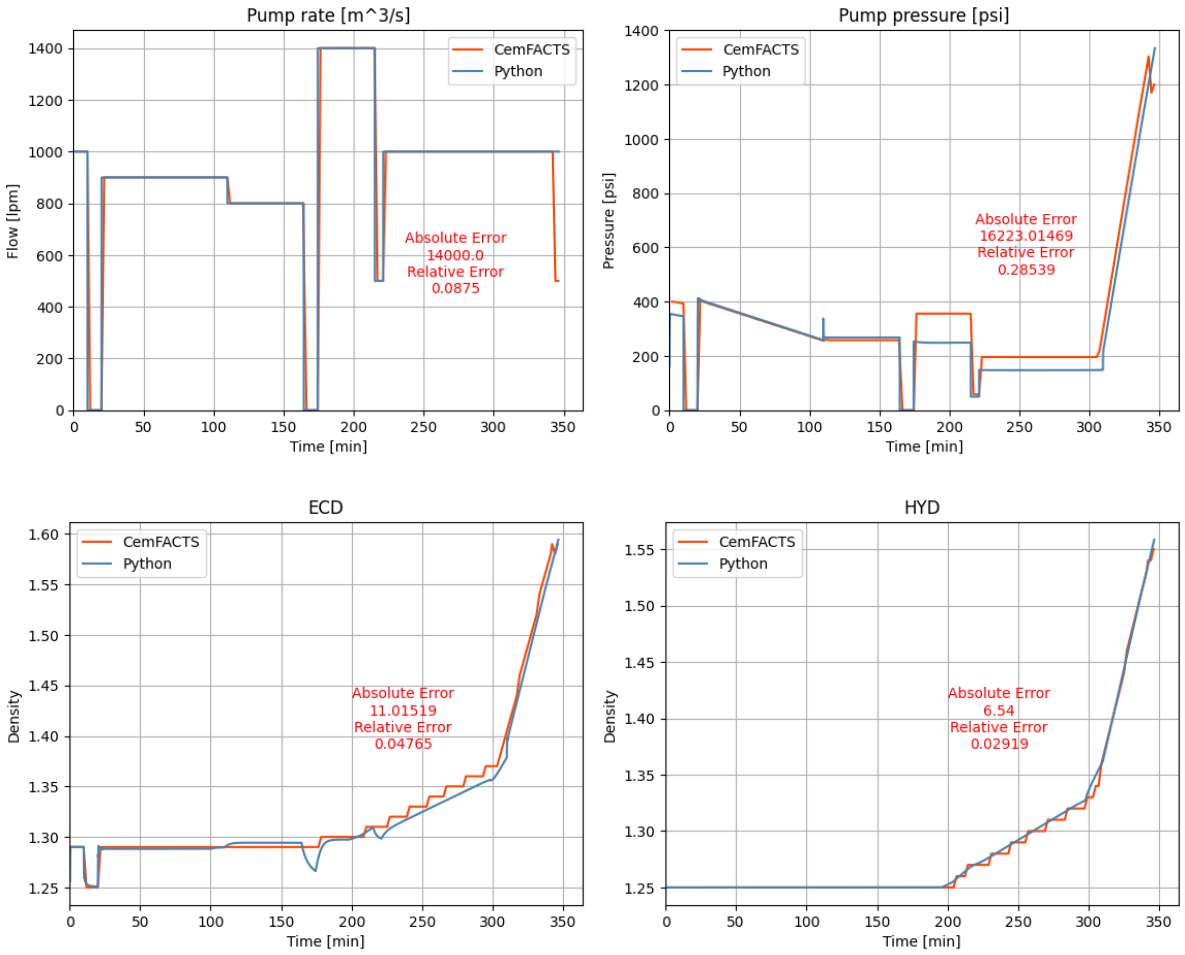

Table IV.9: A different graphs of deferent simulation outputs (Well B)

Although the density curves exhibit high accuracy, the program halts after the CemFact time due to its predefined stop condition. Similar to Well A, the pump pressure graphs display major differences throughout the entire time domain, which we believe are caused by the same underestimation of friction calculations as in the previous well. Detailed results of the annular displacement are presented in **Table IV.4**.

	Lengths (m)		**Volumes (m3)**	
	CemFACTS	**Python**	**CemFACTS**	**Python**
Spacer	0	0	0	0
Lead slurry	1497	1482.92	80.89	80.87
Tail slurry	897	905	43.59	41.64

Table IV.4: Annular displacement (**Well B**)

IV.3 Discussion & Conclusion

In this work, a simplified hydraulic model was developed to describe the pressure and flow dynamics during a well cementing operation. Simulations were conducted using Python, where a conventional cement job code was designed to accommodate four fluids within the casing and annulus, taking the surface line into account as well. The results of these simulations were presented and discussed in terms of several key parameters:

- Pump pressure (psi)
- Flow rate (m^3/s)
- Hydrostatic pressure in the pipe and in the annulus (psi)
- Friction pressure loss the pipe and in the annulus (psi)
- Bottom hole pressure (psi)
- Free fall U-tubing (m)
- Equivalent circulating density at true vertical depth (kg/L)
- Hydrostatic density at true vertical depth (kg/L)
- Lengths of fluids in the pipe and annulus (mud, spacer, lead, tail, displacement mud) (m)
- Volumes of fluids in the pipe and annulus (mud, spacer, lead, tail, displacement mud) (m^3)

The results from the Python simulations for two wells were compared with those obtained from the CemFACTS simulator version 6.3. The study led to several important conclusions:

- The performance of the simplified hydraulic model was demonstrated with unified rheological model employed to determine friction pressure losses, including those in transitional and turbulent flow regimes.
- **The effect of free-fall** was incorporated into the hydraulic model. During the free-fall period, the return rate can exceed the pump rate at the surface, potentially being misinterpreted as a kick. Conversely, when the discontinuous gap decreases (as fluid from the rig pump fills the gap), the return rate can fall below the rig pump rate, which might

be mistaken for a loss to the formation. These varying flow rates cause fluctuations in the bottom hole pressure (BHP), which is critical to minimize, especially in narrow operational pressure windows. Additionally, as long as the discontinuous gap exists, no surface pressure readings are available, reducing the operator's control over the operation.

- **The equivalent circulating density (ECD)** must be maintained above the pore pressure gradient to prevent influx and below the fracture pressure gradient to avoid losses to the formation. A major challenge during cementing is managing these formation losses. Both hydrostatic and frictional pressures can increase rapidly during the displacement of the spacer and cement into the annulus, potentially fracturing the formation. This work highlights the capability of the simplified hydraulic model to simulate well cementing operations effectively. Despite some differences compared to simulators like CemFACTS, which we think this version of the software may use simpler formulations or criteria due to slow variations over time steps, Our model remains robust.

There are several aspects of this thesis that could benefit from further refinement and additional research. Below are some recommendations for future work:

1. **Dividing Flow Sections for Improved Accuracy**: To enhance the precision of flow calculations, it is recommended to divide the flow sections into smaller segments, similar to the approach used in computational fluid dynamics (CFD). By iterating through these smaller sections, the precision of flow calculations can be significantly improved, leading to a more accurate overall model.
2. **Accounting for Temperature Effects Downhole**: Expanding the model to include the effects of downhole temperature variations would provide a more comprehensive analysis. By incorporating temperature variations, a better understanding of the conditions and behaviors within the wellbore can be achieved. This would enable a more accurate prediction of the wellbore's performance under different thermal conditions.
3. **Utilizing High-Performance Libraries**: Employing high-performance computational libraries can significantly reduce the manual effort required for complex calculations. These libraries are optimized for efficiency and can handle the computationally intensive tasks, allowing researchers to focus on the analytical aspects of the work like **FluidDyn** project. By leveraging these libraries, the overall workflow can be streamlined and the computational accuracy can be enhanced.

Figure IV.10: FluidDyn project logo

General conclusion

This study demonstrates that developing a program based on fluid rheology is challenging and requires extensive research to build the necessary knowledge to solve such a complex problem. However, it also proves that relying on the personal results of researchers can lead to performance comparable to departments of major companies, such as the Pressure Pumping Software Applications department of Baker Hughes, which develops high-performance software like CemFACTS.

Our journey to this point has been filled with obstacles. From a technical perspective, it has provided us with a more theoretical understanding of cementing operations, though it revealed significant weaknesses in other aspects of these operations that are crucial. We believe that we have pioneered this path, and we are willing to offer advice to those who seek it, rather than to those who have only observed from a distance.

As a subject for a master's degree thesis, this topic may not be the best choice. This field of study requires substantial resources to foster innovation, and the level of scientific advancement in our universities is not sufficiently developed to push the limits in this area. Therefore, we recommend choosing a more practical topic to gain a broader practical perspective that can enhance your experience and improve your job prospects.

LIST OF REFERENCES

[1] Liu, G. (Ed.). (2021). Applied well cementing engineering. Gulf Professional Publishing.

[2] Nelson, E. B. (Ed.). (1990). Well cementing. Newnes.

[3] Alberta Energy and Utilities Board: "Statistical Series 57, Field Surveillance April 1998/March 1999, Provincial Summaries," http://www.eub.gov.ab.ca/bbs/products/ STs/st57-1999.pdf (accessed October 10, 2005).

[4] - Dargaud.B.D and Boukhelifa.L, "Laboratory Testing, Evaluation, and Analysis of Well Cements",

[5] - Geoge O. Suman, Jr. and Richard e. Ellis, "Cementing Oil and Gas Wells", World Oil (1977).

[6] -Zheng, G., Guo, X., Li, Z., & Sun, J. (2021). Design and evaluation of high-temperature well cementing slurry system based on fractal theory. Energies, 14(22), 7552.

[7] - Moreira, R. P., Ribeiro, D. B., Lima, L. B., & Piedade, T. S. (2023, October). Quality Assurance on Annulus Isolation Under Well Cementing Uncommon Events–Practical Approaches in Deepwater Wells. In Offshore Technology Conference Brasil (p. D031S038R005). OTC.

[8] - Wilson, D. I. (2018). What is rheology?. Eye, 32(2), 179-183.

[9] - *Encyclopedia Britannica*, "Viscosity", *26 June 2023*.

[10] - Chhabra, R. P., & Richardson, J. F. (2011). Non-Newtonian flow and applied rheology: engineering applications. Butterworth-Heinemann.

[11] - Peker, S. M., & Helvaci, S. S. (2011). Solid-liquid two phase flow. Elsevier.

[12] - Lauzon, R. V., & Reid, K. I. G. (1979). New rheological model offers field alternative. Oil and Gas Journal, 77(21), 51-57.

[13] - Marshall Cavendish, *"3*Growing up with Science". *2006. p. 1928.* ISBN ----978-0-7614-7521-7.

[14] Sekhavat, P., Sepehri, N., & Wu, Q. (2006). Impact stabilizing controller for hydraulic actuators with friction: Theory and experiments. Control Engineering Practice, 14(12), 1423-1433.

[15] Wen, J., & Lian, Z. (2011). The communication protocol design of electro-hydraulic control system for hydraulic supports at coal mine. In Web Information Systems and Mining: International Conference, WISM 2011, Taiyuan, China, September 24-25, 2011, Proceedings, Part I (pp. 73-78). Springer Berlin Heidelberg.

[16] – Øyvind Nistad Stamnes, Erlend Mjaavatten and Kristin Falk, "A Simplified Model for Multi-Fluid Dual Gradient Drilling Operations", 2012.

[17] - Glenn-Ole Kaasa, Øyvind Nistad Stamnes, Lars Imsland and Ole Morten Aamo, "Simplified Hydraulics Model Used for Intelligent Estimation of Downhole Pressure for a Managed-Pressure-Drilling Control System", 2012

[18] - Isambourg, P., Anfinsen, B. T., and Marken, "Volumetric Behavior of Drilling Muds at High Pressure and High Temperature. Paper presented at the European Petroleum Conference", 1996

[19] – Goodson, R. E., and Leonard, R. G. , "A Survey of Modeling Techniques for Fluid Line Transients", 1972

[20] - Stecki J. S., Davis D. C., "Fluid transmission lines—distributed parameter models. Part 1: A review of the state of the art", 1986

[21] – Petersen, W., and J. McPhee , "Comparison of Impulse-Momentum and Finite Element Models for Impact between Golf Ball and Clubhead", 2008

[22] – Faith A. Morrison, "Data Correlation for Friction Factor in Smooth Pipes", 2013

[23] – K. M. Assefa and D. R. Kaushal, "A comparative study of friction factor correlations for high concentrate slurry flow in smooth pipes", 2015

[24] – Kamel, A. H., Shaqliah, A.S., and Ibrahim, "Model Inference using the Akaike Information Criterion for Turbulent Flow of non Newtonian Crude Oils in Pipelines", 2015

[25] - Rudman, M., Blackburn, H. M.,Graham, L., and Pullum, "Turbulent Pipe Flow of Shear-Thinning Fluids", 2004

[26] – Ahmed H. Kamel, Ali S. Shaqlaih and Arslan Rozyyev, "Which Friction Factor Model Is the Best? A Comparative Analysis of Model Selection Criteria", 2018.

[27] - El-Emam, N. Kamel, A. Al-Shafie, and Al-Batrawi, "New Equation Calculates Friction Factor for Turbulent Flow of Non-Newtonian Fluids", 2003.

[28] - Mario Zamora, Sanjit Roy and Ken Slater , "Comparing a Basic Set of Drilling Fluid Pressure-Loss Relationships to Flow-Loop and Field Data", 2005

[29] - Mario Zamora , "Virtual Rheology and Hydraulics Improve Use of Oil and Synthetic-Based Muds", 1997